

TEST AND FATIGUE OF THE RAIL

S. KECSKÉS

Department of Railway Construction.
Technical University, H-1521 Budapest

Received October 3, 1985

Abstract

The rail as the most significant element of the railway track has been developed even in recent decades both in relation with its mechanical and chemical parameters. The evolution in testing the different steel materials permits to establish results in behaviour which are not specified by norms and their detailed calculation. Such is, e.g., the impact work as well as the determination of the transition temperature which in relation with the continuously welded rails (c.w.r.) might become a necessary requirement. The transition temperature of the rail steels in dependence on their mechanical and chemical properties is also dealt with by the paper. It has been established that the transition temperature of the rails currently used is very high and, consequently, the process of recrystallization does not take place at all in the case of the rails lying in the railway track. The steels of rail are to be classified in the brittle or in the transition zone of fracture. This circumstance ought to be changed in order to be able to reduce the rail failures and weld ruptures in winter time. The fatigue cracks in the rail, their propagation and the classification of these cracks under the safety limit is of importance from the point of view of a safety railway operation. The author investigates the occurrence of such deficiencies under the safety limit as well as the time-dependent propagation of them and gives answers to the questions relating to the classification and development of the kidney-formed cracks caused by the fatigue of the rail steel, further he points out the position, form, extension and the fracture surface. In justifying the supersonic test of fatigue cracks presents its mathematical formula in dependence on the load.

Table of content

1. Preface, development of the rail
2. Damages in c.w.r. tracks occurring in connection with the rail
3. Change in steel behaviour with the drop of the temperature
 - 3.1 Examination of the critical temperature for the brittle fracture
4. Chemical analysis of the rails examined
5. Examination of the mechanical behaviour, the micro and macro structure and hardness of the rails
 - 5.1 Macroanalysis of the rails
 - 5.21 Baumann's print
 - 5.22 Deep-etching
 - 5.23 Hardness of rails examined
6. The Charpy impact value of the rail steels and the transition temperatures of rails
 - 6.1 Interdependence between the transition temperature and tensile strength (R_m and σ_B respectively)

7. Fatigue test of rails

7.1 Selection of the stress steps in testing the rails for their service life, and the results obtained

8. The origin and propagation of fatigue cracks in the rail head

8.1 The fatigue oval flaw and failure in the rail head

8.11 The conditions of propagation of the fatigue crack in the rail steel

8.2 Location, form and size of the fatigue oval flaws and the fracture surface

8.3 Establishment of the extent and calculation of the flaw with the aid of ultrasonic testing

8.4 Development and calculation of the fatigue oval flaw in dependence on the gross ton load

1. Preface, development of the rail

The rail is the most significant and most characteristic element of the railway track which, through the contact with the wheels of vehicles, receives the axle-load, transmits it to the other elements of the track and lastly to the substructure. Beside this, the rail sends the inducing effect of the track to the vehicle.

The development during the last decades brought to the surface a lot of new problems but it is also of importance that the examination of the movement of the vehicles essentially is restricted to the interaction between the rail and wheel.

In investigating the damages occurring in the track one should set out from the different effects applied on the track by the vehicles moving on it. The way of moving of the wheel set of the vehicles on the track is affected by several factors which are as follows:

- the geometry and grading conditions of the track,
- the state of the track and the vehicles,
- the shape of the wheel rolling along on the rail, and the profile of this latter,
- the displacement of the wheel set in the axle guard,
- aligning ability of the bogies,
- characteristics to swinging (suspension of the vehicles, shock absorption, mass distribution, wheel load),
- weathering conditions,
- speed, etc.

At the end of the 1960s also the Hungarian railways have begun to develop the tractive vehicle stock by which the axle load of the tractive engines became heavier, the axle arrangement significantly changed, also the speed of the

vehicles has been increased. Unfortunately, the state of wheels of the vehicles became, in general, worse (the number of flat wheels augmented, the deposition of the material of the brake blocks to the wheel tread multiplied, etc.), in consequence of which the behaviour of the track also changed. Although the vertical wear of the rails did not become worse, in curves the side wear of the railhead in the rail of greater radius became stronger. A demand for a better rail material has been raised with the view to improve the dynamics and safety of running.

Due to such a diversity of functions and the increased stresses induced in the rail, it became many times one of the most significant subjects of research investigations during the evolution of the railways as it is ever in our days. Our predecessors but also the specialists of our days had examined, and examine continuously the shape, mass, chemical composition, mechanical behaviour and last but not least the possibility of its applicability.

In the course of more than a century the change in the results of the research investigations could not lead to a definite solution of the problem. However, the research for an optimum or the hope or faith in finding the best, resulted for a while in an apparent acquiescence. In searching for better parameters for the rail the decisive factors remained always the manyfold stresses induced in the rail by the load, in connection with the safe operation and the demand for the reduction of the time and costs needed to the track maintenance which latter becomes ever more significant.

To the changes of the different parameters in the course of the development of the rail, *Table I.* gives a short survey. The change in the mass of the rail followed the increase of the axle load and the speed. The augmentation of the axle load demanded the increase of the tensile strength of the rail steel. As a matter of course, to all these also the upgrading of other structural elements of the track and a great number of potentialities given by the progress in engineering technique has been added.

In connection with the material of the rail lying in the track can be assumed to be ideally homogeneous. However, this assumption is justified only in case where one leaves out of consideration the structure and microproperties of the rail steel and one takes the rail as a whole unit unchangeable in its cross section which otherwise would also be justified from the user's point of view.

However, in practice, different faults and deficiencies can be found in the fields of the production and utilization of the rail. The objective to be attained is to eliminate or, at least to reduce the occurrence of these defects. It would be favourable to be able to justify that the rails coming out from the works are of sound, homogeneous structure and faultless composition. To perform the examination in that connection up-to-date engineering equipments and instruments are at disposal, without which one could not be persuaded of the quality of the rail material. The statistical methods cannot replace the instrumental examinations they can only complement them.

Table I
Complete program

Out/In LRN				
1 2 nd Σ +	17 2 nd Lbl 1	27 2 nd Lbl 2	36 2 nd Lbl 3	53 2 nd Lbl 4
2 R/S	18 SBR 0	28 SBR 0	37 RCL 4	54 RCL 1
3 RST	19 X	29 X^2	38 Y^x	55 X
4 2 nd Lbl 0	20 INV 2 nd \bar{X}	30 :	39 RCL 1	56 RCL 2
5 RCL 5	21 +/-	31 2 nd σ^2	40 X	57 :
6 :	22 +	32 X	41 RCL 2	58 [
7 RCL 0	23 2 nd \bar{X}	33 INV 2 nd σ^2	42 =	59 RCL 1
8 -	24 =	34 =	43 +/-	60 -
9 2 nd \bar{X}	25 INV 2 nd log	35 INV SBR	44 INV In X	61 1
10 X	26 INV SBR		45 +/-	62]
11 INV 2 nd \bar{X}			46 +	63 =
12 =			47 1	64 2 nd log
13 :			48 =	65 :
14 INV 2 nd σ^2			49 X	66 RCL 1
15 =			50 RCL 3	67 +/-
16 INV SBR			51 =	68 =
			52 INV SBR	69 INV 2 nd log
				70 INV SBR

Complete erasing 2nd INV C.t

Input of data $X_i \rightarrow X < t; Y_i \rightarrow R/S$

calculation of slope	calculation of the point of intersection on the X-axis	calculation of the coefficient of linear correlation	calculation of KV/T/	calculation of TT
$n \equiv m = \text{SBR } 0$	$k \equiv b = \text{SBR } 1$	$r^2 \equiv \text{SBR } 2$	$n \rightarrow \text{STO } 1$ $k \rightarrow \text{STO } 2$	$\text{TT} \rightarrow \text{SBR } 4$ $\text{STO } 4$
		$r \rightarrow \sqrt{\bar{X}}$	$\text{KV max.} \rightarrow \text{STO } 3$ $T_i \rightarrow \text{STO } 4$ $\text{KV (T)}_{sz} \rightarrow \text{SBR } 3$	$\text{TTKV} \rightarrow \text{SBR } 3$

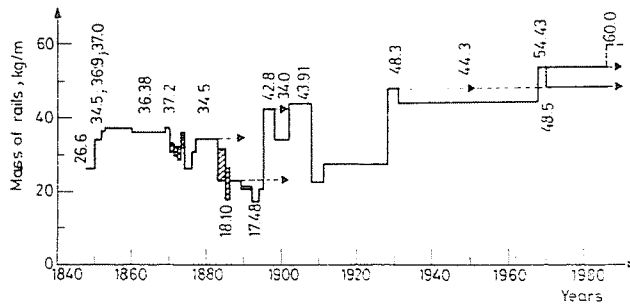


Fig. 1. Rails produced for the lines of normal gauge of the Hungarian railways with the years of introduction (1840—1984)

The stress generated in the rail can be of several origins (manufacturing, load, etc.). The stress caused by the change of the rail temperature in the c.w.r. track is significant. The changes of the internal stresses caused by the changes of temperature, are higher than those which occur in tracks constructed in the traditional way (e.g., the tensile and compression forces).

Under the effect of the continuously changing temperature the behaviour of the rail steel also is changing. Although these changes have been studied already in adopting the c.w.r. tracks and in the course of research investigations undertaken since then, however, this has been done only in an inextensive way. It has been revealed that the reduction of the impact work under the effect of low temperature in winter and, at the same time, the increased tensile stress developed in the rail steel of the c.w.r. track have a particularly high significance.

With the drop of temperature the impact work of most kinds of steel changes unfavourably. The impact work at the temperature of the rail which is characteristic to the kind of the rail steel suddenly decreases within the operation interval of the rail temperature, and the steel grows rigid.

In examining the impact work of the rail steel, the changes taking place in the track, the effects of the rail temperature induced in the tracks laid with c.w.r.s, should be taken into account. Neither the additive effects of the different ingredients entering in the composition of the rail steel should be neglected (Fig. 2). The tensile strength and the impact work of the rail steel are the ever more significant properties of the rail and, in connection with the tensile strength, the wear resistance, which, at the same time is also an economical problem.

The development of the rails used in the network of the MÁV, the mass and other preferable parameters of the rail is demonstrated in Fig. 3 from the beginning of the Hungarian rail construction up to these days.

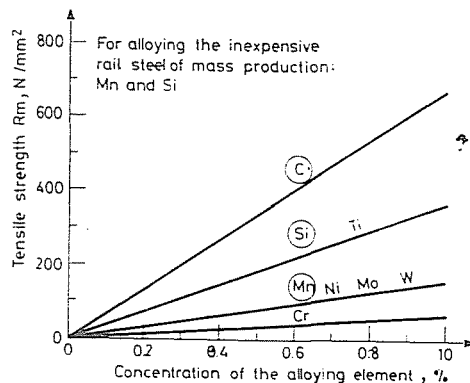


Fig. 2. Effect of the significant alloying elements increasing the tensile strength of the rail steel

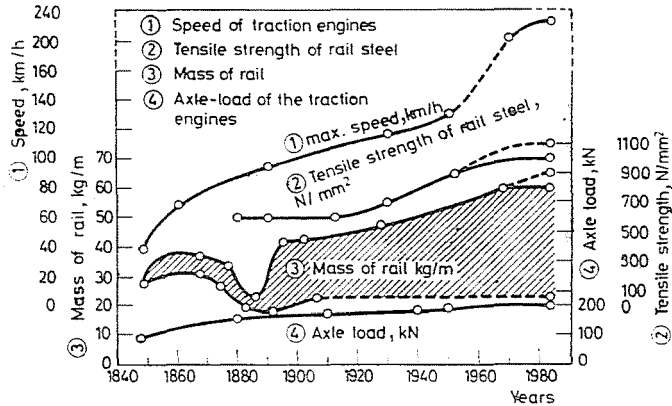


Fig. 3. Changes in the parameters of the rail and traction engines of normal gauge (1840—1984)

At the beginning of the railways the rails have been produced by casting. This technique has been followed by the process of rolling of rails, however, as a matter of course, with an increased unit mass. This finally resulted in adopting the rail system UIC 54. The Hungarian railways have in view, due to the further probable increase in vehicle loads, to adopt the rail UIC 60.

In this connection it is worth-while to take in the situation of the development of the axle-load of the tractive engines (Fig. 4). The effect of the change of the rail and axle-load can unequivocally be pointed out. Examination at the same time of the Figs 1, 3 and 4 justifies that an essential change in the axle-loads and speed of vehicles periodically involves also the increase of the mass of rails. Augmentation of the axle-loads is in the near future not intended but the introduction of higher speeds is an absolute necessity if the rail transport wants

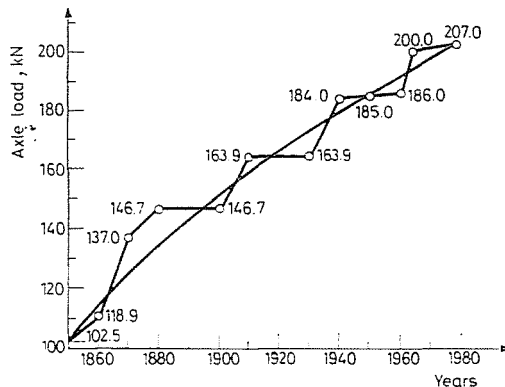


Fig. 4. Change in axle load of traction engines (1850—1984)

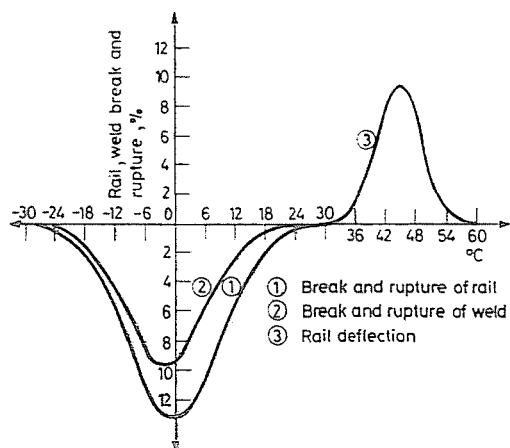


Fig. 5. Break and rupture of rail and weld respectively and track deflection in c.w.r. lines (1960—1980)

to hold its ground in the competition with other transport modes. It may be assumed that the rails UIC 54 and 60 meet the requirements of the higher speed; at most, the mechanical qualities of the rail steel have to be upgraded. The high speed demands rails of high quality of a steel moderately prone to embrittlement, wear resistant and of course a careful maintenance. The rail produced from a wear-resistant steel has also a higher tensile strength but in turn, it has a higher proneness to brittle fracture. Therefore, the failure or rupture of rails, i.e., welds as well as the buckling of the track in dependence on the rail temperature became here the subject of research investigations.

2. Damages in c.w.r. tracks occurring in connection with the rail

Under the climatic conditions of our country the rail temperature changes between -30°C and $+60^{\circ}\text{C}$, just like in the most European countries. In the c.w.r. tracks, in conformity with the above values of the rail temperatures, the rail steel is brittle and finds itself in the transition fracture zone.

The tough fracture zone is far above 60°C , wherefore, the relaxation process, in case of the rail steel does not take place within the temperature interval characteristic to the climate under the effect of the fluctuation of stresses sometimes also failure of the rail and the welds, and the track can also be deflected.

In examining deficiencies of such character, it can be stated that within the boundaries of the rail temperature their occurrences follow the pattern of the Gaussian normal distribution (Fig. 5).

The fracture and rupture of the rail, i.e., the welds, occur within the temperature region between $-30^{\circ}\text{C} \dots +30^{\circ}\text{C}$. The maximum ordinates of the rail fractures and weld ruptures occur at the temperature 0°C . The Gaussian distribution verifies that below the transition temperature characteristic to the rail quality the occurrence of the deficiencies is frequent which is in close connection with the tensile strength of the rail steel.

In the course of the mathematical statistical examinations, the investigation of the fitness and normality undertaken on the basis of the data disposable justified the above statements.

The expectation value m^x is given by the formula

$$m^x = \frac{1}{n} \sum_{k=1}^n v_k \cdot X_k$$

The formula of the scatter which is the density function of the normal distribution, reads:

$$\sigma^{x^2} = \frac{1}{n} \sum_{k=1}^n v_k (X_k - m^x)^2 - \frac{h^2}{12}.$$

The normality examination with the proof of χ^2 is given by the formula:

$$\chi^2 = \sum_{i=1}^n \frac{(v_i - n \cdot p_i)^2}{n \cdot p_i}$$

wherein:

- n — number of measurements,
- p_i — theoretical probability of occurrence of event A_i
- v_i — frequency of events A_i according to the measurements,
- X_i — measurement results,
- m_x — corrected empirical expectation value calculated from measurements,
- $\frac{h^2}{12}$ — Sheppard's correction.

Numerical values of the examination results obtained in case of 405 rail failures:

— expectation value	$m^x = 0.074$
— scatter	$\sigma = 3.034$
— the χ -proof	$\chi^2 = 35.041$
from the table	$\chi^2 = 39.03$

$P(\chi^2 < \chi_0^2) = P(35.041 < 39.03) = 99.9$ percent, where the degree of freedom is 16.

Examining the region of temperature of the track deflection on the basis of its occurrence (Fig. 5), it can be stated that the temperature interval is

39°C . . . 56°C with the max ordinate at the temperature 44.5°C. The 45 per cent of the deflections occur between 32°C and 44.5°C while the 55 per cent take place above 44.5°C. The max. rail temperature does not occur frequently, wherefore the occurrence of the track deflection decreases.

The calculations yield the following numerical data :

$$\begin{array}{ll} m^x = 0.634 & \sigma = 4.227 \\ \chi^2 = 17.330 & \chi_0^2 = 24; \end{array}$$

with a degree of freedom 17.

$$P(\chi^2 < \chi_0^2) = P(17.33 < 24) = 99.0 \text{ per cent.}$$

The distribution of the fractures and ruptures of the welds is similar to those mentioned above (Fig. 5) with the exception that the maximum ordinate falls in the region of the negative temperature and is to be found at $-1 \dots -1.5^\circ\text{C}$.

Numerical data of the calculations are as follows:

$$\begin{array}{ll} m^x = 0.109 & \sigma = 4.125 \\ \chi^2 = 49.634 & \chi_0^2 = 50.892 \end{array}$$

with a degree of freedom 30.

$P(\chi^2 < \chi_0^2) = P(49.634 < 50.892) = 99.0$ percent. The result of the proof χ^2 would be still more favourable in case of the reduction of the temperature values, however, such an examination is not necessary because the distributions are normal and the reduction would result in larger intervals of temperature, in turn, the intervals of larger widths would decrease the actual temperature boundaries of the rail.

Also the distribution of the damages according to the external temperature in the different months proves the lawfulness obtained from the transition rail temperature. This can be brought into connection with the \pm change of the rail temperature and the negative region. The occurrence of the rail and weld failure according to the months listed is as follows:

— November	13.1 per cent
— December	26.7 per cent
— January	26.7 per cent
— February	11.7 per cent = 78.2 per cent

and commonly 21.8 per cent in the early fall and springtime.

According to the climatic conditions of Hungary within the rail temperature interval the 43.3 per cent fall in the brittle and the 56.7 per cent in the zone of the transition failures.

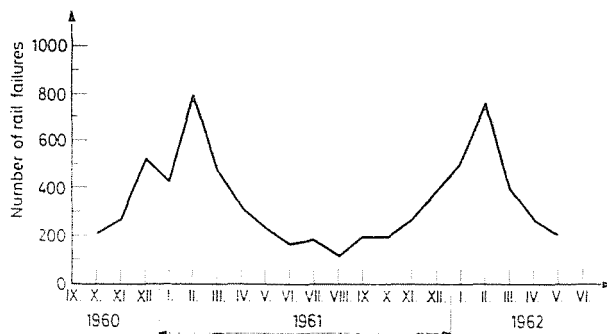


Fig. 6. Development of rail failures observed on the railway lines of the German Federal Republic in 1961

The above statements made in connection with the fractures and ruptures of rails seem to be proved by the numbers of rail failures observed in 1961 on the lines of the German Federal Railways as is to be seen in Fig. 6. The data of the GFR agree according to the calendar with those indicated for the Hungarian railways. The interconnection between the rail failures and the rail temperature have been analysed on the basis of the data of the first two months of the year (Fig. 7). Also this analysis confirmed the issues of our extensive investigations.

The transition temperature of the rail steels are to be examined in the future in a more elaborate way. It is needed especially in the interest of the safety of the railway operation in the field of the track survey services. The rail and weld failures occurring on the railway network require to perform such investigations.

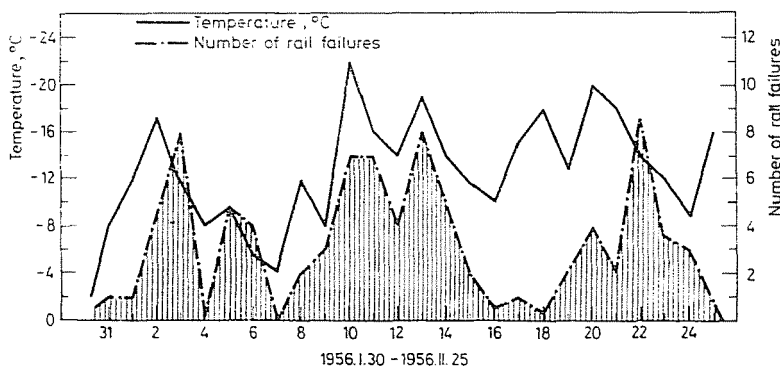


Fig. 7. Interdependence between rail failures observed on the railway lines of the German Federal Republic and the rail temperature

3. Change in steel behaviour with the drop of the temperature

It is known that most of the properties of the steel change with the drop of the temperature. From among the mechanical characteristics there are the tensile strength, the yield point, the limit of elasticity and fatigue as well as the hardness which are increasing with the drop of the temperature, but the contraction and strain of the steel behave in different ways: according to the kinds of steel they remain unchanged or reduce in a moderate or more rapid way. The drop of the temperature affects in the strongest way the impact work of the steel.

The impact work of most types of steel does not reduce proportionately with the decrease of the temperature; it rapidly decreases at a temperature, i.e., temperature interval characteristic to the kind of steel in question; the steel embrittles. This rapid embrittlement is not characteristic. The temperature causing the embrittlement of the steel is called transition temperature. Below this the steel is inclined to brittle fracture. This means that under certain circumstances a tensile stress significantly lower than the strength of the steel cannot be withstood by the steel, it suddenly breaks.

The embrittlement is a reversible process, the steel which has embrittled at a lower temperature recovers its toughness at a higher. This process takes place in case of the rail in the region of temperatures being specific to the climate in question.

For the preservation of the safety of the railway operation the circumstances and extent of the stress have to be in accordance with the toughness of the rail steel which can be revealed by the impact work and not by the aid of the impact test.

The specimens after breaking them by impact tests at different temperatures, show fractures at a certain temperature and above that on the whole cross section of tough pattern. In reducing the temperature of the test, the impact work also reduces and at some cross sections, beside the tough fracture also brittle fracture of crystalline character occurs. If the temperature drops, the area of the crystalline fracture increases and, at a certain temperature and below that the fracture will be brittle on the whole cross section; the specimen will break under the effect of a relatively low load (Fig. 8).

The curves of the transition from the tough to the brittle fracture and the change of the impact work determine three remarkable temperatures (Fig. 9).

T_2 — At a temperature higher than T_2 the impact work of the steel is rather great, the steel is tough, it is capable to withstand a load heavier than that causing a stress higher than the elastic limit with plastic deformation and cracks do not rapidly propagate.

TT — The transition temperature of the steel which falls in the interval of the transition fracture, the point of inflection is the middle point of the field.

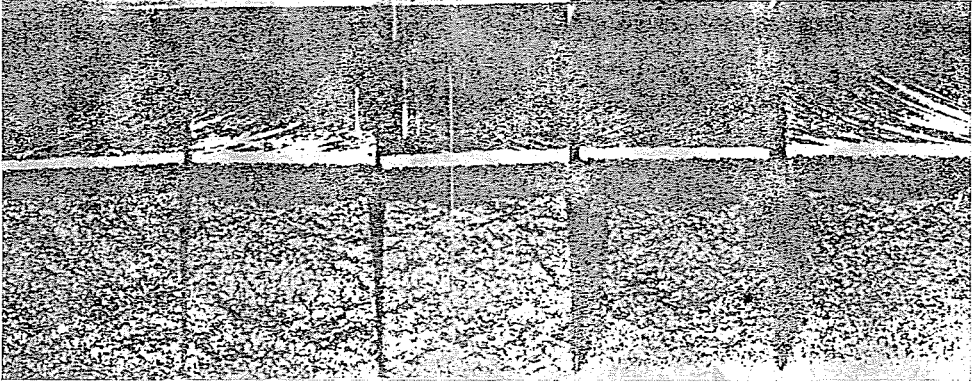


Fig. 8. Photo of fractures taken of the VGB impact tests performed on GFR rail

T_1 — At a temperature lower than T_1 the impact work of the steel is small, the steel is almost entirely brittle, wherefore, an initial crack propagates under the effect of a comparatively easy load freely, with a fracture of crystalline surface. The temperature T_1 is called also the temperature of the zero plasticity.

In case of the rail it is to be made commonly allowance for a temperature lower than T_2 under the Hungarian climate to 60°C which is here the highest temperature. $T_{60} < T_2$.

Within the interval between T_1 and TT , the steel must not be submitted but to a static load inducing a stress lower than the elastic limit. A stress surmounting the elastic limit can initiate crack or even failure and, under the effect of a dynamic load an initial crack of any origin causes fracture.

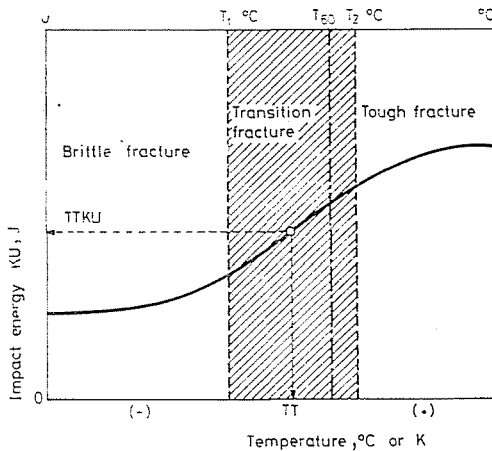


Fig. 9. Change of the impact energy of the steel and the nature of the fracture in dependence of the temperature

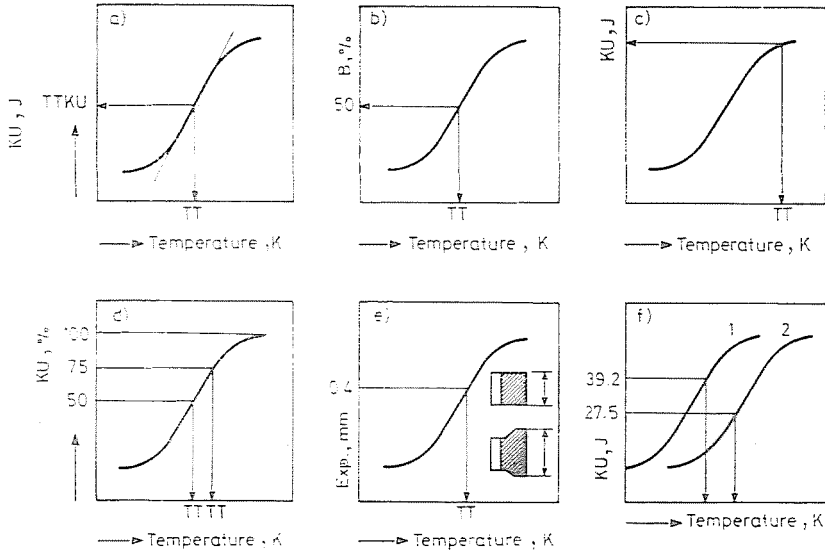


Fig. 10. Procedures of determinations of the transition temperature

3.1 Examination of the critical temperature for the brittle fracture

The temperature of the transition from the tough state of the steel into the brittle is examined by impact bending test. To the determination of this state of transition no uniform method has been so far developed.

To the definition of the transition temperature the following conventions have been as yet made (Fig. 10).

The transition temperature is:

- according to the impact work the temperature associated with the point of inflection of the rail temperature (Fig. 10a);
- the rail temperature at which the fracture of the specimen is up to 50 per cent of tough character (Fig. 10b);
- the rail temperature at which the rail material ceases to be toughed up to 100 per cent (Fig. 10c);
- the rail temperature at which the impact work reduces in comparison with the tough state by 25 or 50 per cent (Fig. 10d);
- the rail temperature at which the expansion of the specimen decreases under 0.4 mm (Fig. 10e);
- depending on the yield point of the material up to the yield point $R_{eH} = 300$ MPa the temperature coordinated to the impact work 27 J;
- above the yield point $R_{eH} = 300$ MPa the temperature coordinated to the impact work 40 J (Fig. 10f).

The literature on the subject dealing with the critical temperature of the brittle fracture offers numerous mathematical formulae to the solution which, however, are intricate mathematical relationships or empirical methods.

The formula chosen can be calculated with the aid of simple means by using the method of linear regression. To this purpose, in choosing the temperature interval, the reliable measurement points near the transition temperature should be assured by a careful planning. Also the maximum of the rising branch of the curve has accurately to be defined.

The curve KU-T defined with the aid of regressive calculation will be utilizable to determine the value of the critical temperature of the brittle fracture defined in several ways (Figs 10a, c, d, f). The method can be used also by an appropriate transformation of the parameter Y_i to the examinations based on the ratio of the tough fracture surface (Fig. 10b) and the measurement of the cross swelling of the specimen (Fig. 10c).

One part of the tentative standards suggest to the determination of the transition temperature the simultaneous application of several conventions.

In the course of the impact-bending tests performed at different examination temperatures the relationship

$$KU = f(T)$$

results in a curve of a characteristic S-form.

In the domain within the minimum and maximum impact-work values the curve can be closely approached by AVRAMI's formula known in connection with the phase transformation

$$Y = 1 - \exp \cdot (-k \cdot T^n). \quad (1)$$

For materials of the same state in case of identical test conditions, the results obtained from a series of tests an equation can be established which fits in a similar way the above formula:

$$KU(T) = KU_{\max} [1 - \exp \cdot (-k \cdot T^n)] \quad (2)$$

wherein:

- T — temperature of examination (K°),
- $KU(T)$ — impact-work value calculated (J),
- KU_{\max} — maximum value of impact work (J),
- k, n — constant values.

Given that Eq. 2 can be linearized, it can be applied also to regressive calculation:

$$\frac{KU(T)}{KU_{\max}} = 1 - \exp(-kT^n)$$

$$\frac{KU_{\max} - KU(T)}{KU_{\max}} = \exp(-kT^n)$$

$$-\ln \frac{KU_{\max} - KU(T)}{KU_{\max}} = k \cdot T^n$$

$$\lg - \frac{\ln KU_{\max} - KU(T)}{KU_{\max}} = \lg k + n \cdot \lg T \quad (3)$$

$$Y = mX + b$$

By making use of Eqs. (4) and (5) the constants of Eq. (3) can be calculated using the method of linear regression:

$$n \equiv m = \frac{\sum_{i=1}^t X_i \cdot y_i - \bar{X} \cdot \bar{y}}{\sigma_x^2} \quad (4)$$

$$\lg k \equiv b = Y - m \cdot X \quad (5)$$

The equation is derivable. At the zero value of the second derivative the curve has a point of inflexion:

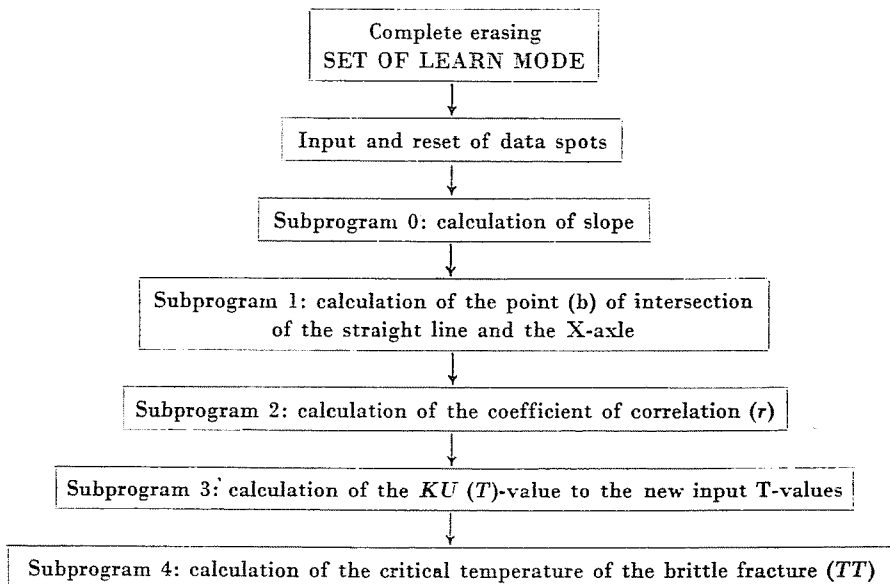
In case of $\frac{d^2 KU(T)}{dT^2} = 0$, from equation (2)

the relationship

$$\lg T = \frac{1}{n} \lg \frac{n-1}{n \cdot k} \quad (6)$$

can be obtained, from which after replacement of the constants at the point inflexion the transition temperature of the brittle fracture (TT) and the critical value of the impact work ($TTKU$) can be calculated.

The flow chart of the program is as follows:



The steps of the complete program are contained by Table I. Calculation of the linear regression can be performed with the aid of a machine type PTK-1050 by a repeated and a machine, type PTK-1072 by a single programming.

4. Chemical analysis of the rails examined

In the course of the examination comparison has been made between rails made in Hungary and some rails of foreign origin with the analysis of the results obtained.

The rails examined are as follows

- System 54, open-hearth iron, produced in Hungary
- System 54, produced in electro-hearth furnace, Hungary
- System 54, converter iron, produced in Hungary
- French rails, system 60
- System 65, made in Czechoslovakia
- Austrian rails, system 60
- System 65, made in the Soviet Union
- System Phönix of the German Federal Republic
- and MÁV 48³ rail made in open-hearth furnace.

The chemical composition of the rails given in weight-percentage is indicated in Table II. The C content of the rails produced with an up-to-date procedure varies between 0.63 and 0.75 per cent. From the point of view of C

Table II
Chemical composition and

Origin and mass kg/m	Elements					
	C	Mn	Si	S	P	Cr
						%
(L K M)						
electro (54)	0.64	1.08	0.24	0.021	0.021	0.12
converter (54)	0.64	1.06	0.25	0.022	0.021	0.10
open-hearth (Martin)	0.63	1.25	0.31	0.035	0.014	0.06
Czechoslovak (65)	0.75	1.16	0.25	0.031	0.022	0.07
French (60)	0.64	1.49	0.38	0.041	0.035	0.02
Austrian (60)	0.67	1.17	0.44	0.031	0.031	0.01
Soviet (65)	0.69	0.93	0.21	0.016	0.018	0.01
GFR (Phönix)	0.53	0.84	0.17	0.031	0.024	0.10
Hungarian, (48) open-hearth steel	0.59	1.00	0.29	0.030	0.020	0.07

content are the Czechoslovakian and Soviet rails to be distinguished (0.75 and 0.69 per cent respectively).

The rail, system Phönix of the GFR and the Hungarian rail system 48³ produced in open-hearth furnace have a C content 0.53 and 0.59 respectively.

The Soviet and the Phönix as well as the Hungarian rail 48³ mentioned above, made in open-hearth furnace are of low carbon content.

The Si content of the Austrian and Phönix rails shows a relatively high deviation, it is above the average in case of the French rail.

The over-all content of S and P surpasses in case of the foreign rails the 0.05 per cent. Cr, Cu and Al occur in a lower weight percentage.

The gas, notably nitrogen content of the Hungarian rails produced in converter or electro-hearth furnace is lower than that of the foreign rails examined, with the exception of the Soviet production, system 65 kg/m.

The elimination, i.e., reduction of the nitrogen content, its damaging effect to the steel, e.g., the "aging" caused by the nitrogen has been significantly decreased, in consequence of which it could be avoided that the steel after a slight permanent deformation or a long time storage would on the normal temperature be embrittled.

The strength of the rail steel can be increased by alloying, heat treatment or by applying both of these procedures at the same time.

As alloying elements molybdenum and vanadium are to be taken into consideration in the first line. The molybdenum besides its high toughness increases the hardness and tensile strength of the steel and ensures a good elas-

gas-content of the rail tested

Ni	Mo	V	Cu	Al	Gas content		
					H ₂	O ₂	N ₂
					ppm		
0.09	0.03	0.01	0.10	0.04	5.63	20.7	25.1
0.06	0.03	0.01	0.08	0.04	6.99	17.0	30.0
0.09	0.03	0.01	0.20	0.11	6.48	12.1	34.8
0.02	0.02	0.01	0.09	0.02	6.06	12.8	34.5
0.03	0.02	0.01	0.03	0.02	5.33	13.5	32.0
	0.01		0.01	0.09	8.36	12.0	35.0
0.02	0.01		0.05	0.01	4.28	34.0	26.0
0.03	0.02		0.03	0.02	5.49	17.0	46.0
0.07	0.03	0.01	0.20	0.05	6.68	35.0	38.0

ticity to it, while the vanadium exercises a grain refining effect and fosters the formation of vanadium carbides.

For the converter rail-steels a low Cu content is favourable since it eliminates the phenomenon of the red-shortness.

According to the quantitative analysis of the rail specimens as to the composition of the rails of different production they meet the specifications of the quality MA2.

5. Examination of the mechanical behaviour, the micro and macro structure and the hardness of the rails

The data obtained by the mechanical examinations are summarized in Table III.

The results obtained by the strength tests of the rails of different production also meet the quality specifications MA2.

According to the specifications mentioned above

$$R_m \geq 880 \text{ MPa}; \quad A_5 \geq 9 \text{ per cent}$$

which requirements are fulfilled.

From among the rails tested, the Austrian, Czechoslovak and French rails have the highest tensile strength. In the composition of these rails, C, Mn, and

Table III

Mechanical parameters of the rails tested (average values of 9 specimens per tests)

Origin and mass kg/m	Yield point	Tensile strength	Con- traction	Strain	$\frac{R_{eH}}{R_m}$	C = $\frac{R_m + 3A_5}{(R_m/kp/mm^2)}$	Grain fraction in the rail head according to ASTM	
	R_{eH_2}	R_m	Z	A_5			at the edge	in the middle
	MPa	MPa	%	%				
(L K M)								
Electro (54)	522	901	28.2	11.6	0.58	127.3	5.1	4.0
converter (54)	511	904	20.4	11.3	0.56	126.1	5.0	4.4
open-hearth (54)	519	928	25.2	10.7	0.56	126.7	4.9	4.2
Czechoslovak (65)	551	942	19.0	9.8	0.58	125.4	5.5	3.6
French (60)	562	933	22.2	12.0	0.60	131.1	4.7	3.0
Austrian (60)	532	952	21.7	12.2	0.56	133.7	6.1	5.3
Soviet (65)	504	894	19.0	12.1	0.56	127.5	5.1	3.6
GFR (Phönix)	420	750	35.2	17.3	0.56	128.4	5.5	4.6
Hungarian, (48)								
open-hearth-steel	493	882	24.0	11.4	0.56	122.4	5.4	4.5

according to the specification of the Hungarian Standard 2570—80: $R_m > 880 \text{ N/mm}^2$
 $A_5 > 9\%$

even Si occur with a higher weight per cent than in the Hungarian rails, which follow the rails mentioned above, the last being the Soviet rail.

The elongation of the rails tested (A_5 per cent) is in case of the Hungarian rails 10 . . . 12 per cent, while that in case of the foreign rails makes up 12 per cent, and this parameter has the lowest value for the Czechoslovakian charge of rail steel with 9.8 per cent, however, also this cypher meets the specifications.

The new norms give no more specification as to the contraction (Z per cent) but, in considering also this value it can be pointed out that it is higher in case of the rails produced from electro and Martin charges having high tensile strength than in case of rails made from other charges. The deviation considering the sum of the tensile strength (Rm) and the threefold value of the strain (A_5 per cent), i.e., $Rm + 3A_5$, is to be found between 1 and 5 per cent.

In essential, the mechanical properties are similar, independently of the origin which may be attributed to the fact that the C content slightly variable is equalized by the alloying elements and impurities of small quantity.

The surplus contraction of the Hungarian rails permits to conclude to the fact that with the aid of thermal control of the rail a higher strength might be obtained without damaging the toughness properties.

5.1 *Microanalysis*

In case of the microanalysis the author restricted himself to the examination of the texture because the rail Phönix excepted, due to the nearly eutoidal composition of the other rails no suitable method has been found to the determination of the grain size.

The texture of all of the rails has been found laminar pearlite with more or less ferrite.

5.2 *Macroanalysis of the rails*

5.21 *Baumann's print*

From all rail specimens, from the cross and longitudinal discs Baumann-prints have been made.

On the discs taken perpendicularly to the rail centre-line the distribution of the sulfur is uniform. On the specimens taken along the centre-line of the rail linear and intermittent enrichments of sulfur have been found.

5.22 *Deep-etching*

The longitudinal and cross-specimens of the rail have been deep-etched. In case of the longitudinal specimens after working off 1 mm layers at both sides, a repeated deep-etching took place until the 25 mm thickness of the floc-

culated disc reduced to 20 mm. An intermittent etching became apparent both on the converter and Martin-steel rails.

Flocculated steel could not be observed at all among the rails examined.

5.23 *Hardness of the rails examined* (Fig. 11)

The hardness has been examined through the whole cross section of the rail with measurements

- in the rail head at 15 (5×3) points in horizontal and vertical directions
- in the web at 8 (vertically),
- in the flange at 9 points (horizontally).

The measurement data have been variable even in the very same cross section of the rail.

In case of the Hungarian rails those made from converter steel the distribution of the hardness was comparatively more homogeneous.

In turn, in case of the rails of electro and Martin-steel, on the tapered part of the flange, the hardness was at some spots of a higher value.

The hardness distribution in the head and flange of the Czechoslovakian rail is nearly the same. The hardness is higher at the extremities of the flange but in the web is lower by as high as 4—22 HB-value than in the head or in the flange.

In the head of the French rail the hardness is lower than in the web and flange. The difference reaches even the value 16—28 HB. The steel is the hardest in the web then, it decreases in the flange and in the head.

In the Austrian rail, the distribution of the hardness is, in general, homogeneous. The hardness is at the extremities of the flange by 5 to 9 HB higher than in its middle part.

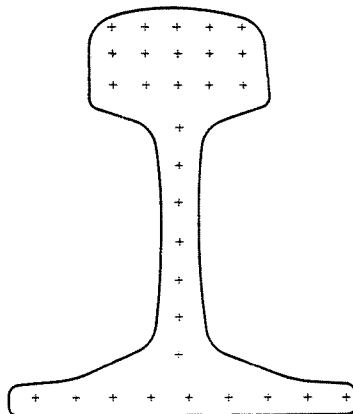


Fig. 11. Spots of hardness measurements HB . . .

In case of a few rails a difference as high as 20 to 22 HB compared to the above values can occur.

The hardest part of the Soviet rail is the head, the hardness in the web and the flange is nearly the same but, in comparison to the values measured in the head is lower by 25 to 32. This favourable deviation is originated from the controlled final temperature of the rolling and from the subsequent careful refrigeration.

6. The Charpy impact value of the rail steels and the transition temperatures of the rails

The measurements of the prismatic notch specimens used to the impact-bending tests were $55 \times 10 \times 10$ mm, the depth of the U-notch was 2 mm ($r = 1$ mm). The highest energy of the ram was 300 Joule.

The Charpy notch impact test specimens have been refrigerated in the mixture of dry ice and denaturated spirit and heated in a desiccator and annealing furnace heating at a low temperature to the test temperature. A relative stability of the test parameters has been realized. Checking of the test results justified the specifications.

The determination of the different conventional transition rail temperatures took place according to Fig. 10.

The averages of the Charpy values are indicated in Table IV. The average values have been established from the results of 16 tests.

The highest Charpy values have been obtained at a temperature 20°C with the specimens of the Martini, converter and electro steels in case of the Hungarian rails. These have been followed by the Austrian and Soviet rails. Values similar to the above mentioned have occurred between the temperatures $-40^{\circ}\text{C} \dots +60^{\circ}\text{C}$ occurring in the track.

The Charpy impact values of the rails examined have consistently been developed at the temperatures lower than -40°C and higher than 60°C . As a matter of course, the Charpy values of the Phönix-rail (GFR) and the Hungarian rails system 48³ kg are higher due to the ferrite network of the basic texture.

The calculation method of the linear regression analysis has been dealt with earlier. The calculated values of the transition rail temperature are summarized in Table 5.

The transition rail temperatures of the Hungarian rails, produced currently, (336 and 334 K) in case of the electro and converter steels are similar to the values of the Austrian rail (334 K). The transition temperature of the Soviet rail (325 K) is beneath those mentioned above while those of the French and Czechoslovakian rails (364 and 358 K respectively) are above them.

The Hungarian rail system 54 of open-hearth steel has a transition temperature (320 K) which is nearly the same as that of the Soviet rail (325 K).

Table IV

Origin	Average* impact-energy values								
	C°	-60	-40	-20	±0	20	40	50	60
	K	213	233	253	273	293	313	323	333
a) Hungarian, syst. 54, open-hearth-steel		7.1	7.8	11.0	14.9	19.6	24.3		25.9
b) Hungarian, syst. 54, electro-steel		7.1	6.3	11.0	11.8	15.0	22.8		28.2
c) Hungarian, syst. 54, conv. steel			8.6	9.4	14.9	17.3	21.2		21.2
d) French rail, syst. 60					7.8	10.2			14.1
e) Czechoslovak rail, syst. 65.					8.6	10.2		11.0	
f) Austrian rail, syst. 60		5.5	7.8	9.4	14.1	14.9	22.0		20.4
g) Soviet rail, syst. 65					9.4	14.9	18.8		
h) GFR Phönix rail		7.8	8.6	20.4	27.5	36.1			41.6
i) Hungarian rail syst. 48 ³		11.6	19.0	21.2	27.1	36.0			40.2

*Averages of tests performed on at least 16 specimens

The transition temperatures of the Hungarian rail system 48³ produced of open-hearth steel (320 K) and of the Phönix-rail (GFR) (295 K) are still lower than the latter.

In the columns of the Table also the different conventional transition temperatures are indicated together with the values KU_{\max} and the Charpy values $TTKU$ (J) associated with the point of inflexion.

In Fig. 12 the places of cut out of the specimens are to be seen.

The curves $KU = f(T)$ of the Hungarian and foreign rails as well as their comparison are represented in Figs 13, 14, 15 and 16.

Calculation of the points of curves $KU = f(T)$ took place according to the procedure described above.

6.1 Interdependence between the transition temperature and tensile strength (R_m and σ_B respectively)

In the course of the extensive examinations performed for the determination of the properties of the different rail steels, also the interdependence between the transition temperature of the rails and their tensile strengths have been investigated.

The investigation of the Hungarian rails took place according to specimens specified by the German norm VGB (DIN 50 115) from the results of which (Fig. 17) is to be seen that the chemical, mechanical, fatigue, etc. behaviour of the Hungarian rails is in close agreement with those of the foreign rails fabricated with the help of up-to-date procedures.

at T_i temperature ($KU_{30/2}$) Joule

80	100	120	130	140	150	180	200	220	250	280	300
353	373	393	403	413	423	453	473	493	523	553	573
25.1	31.4		37.7	39.2	42.4	42.4	43.9			44.7	
30.6	30.6	34.5	42.4	40.8	43.9	46.3	49.4		47.1		
	26.7	29.0	30.6		36.1	43.1	42.4				
	22.8	24.3	24.3	33.0	40.0			43.1	42.4		
	19.6	21.2	22.0	30.6	27.5		33.7		33.7		
22.0	26.7	31.4				42.4	39.2				
	23.5		24.3		34.5						
46.3	51.0				54.9		55.7				
42.5	51.7				71.3		75.9			76.3	

Table V

Calculation of the transition temperature based on actual parameters

Type of rail	KU_{max} (J)	TKU (J)	TT(K) inflexion	TT(K) fracture	TT(K) red	TT(K) 50%	TT(K) 75%	TT(K) exp.	TT(K) 39.2 J
Hungarian, syst. 54, open-hearth-steel	45	24	320 (47)	393 (120)	490 (217)	313 40	374 (101)	373 (100)	415 (142)
Hungarian, syst. 54, electro-steel	49	26	336 (63)	393 (120)	510 (237)	328 55	388 (115)	363 (90)	401 (128)
Hungarian, syst. 54, conv. steel	43	23	334 (61)	393 (120)	530 (257)	328 55	392 (119)	403 (130)	450 (177)
French rail, syst. 60	43	24	364 (91)	403 (130)	480 (207)	354 81	399 (126)	413 (140)	440 (167)
Czechoslovak rail syst. 65	34	18	358 (85)	403 (130)	540 (267)	351 78	412 (139)	413 (140)	—
Austrian rail, syst. 60	42	22	334 (61)	393 (120)	520 (247)	329 56	396 (123)	403 (130)	470 (197)
Soviet rail, syst. 65	35	17	325 (52)	403 (130)	550 (277)	326 53	404 (131)	403 (130)	—
GFR Phönix rail	56	31	295 (22)	293 (20)	400 (127)	287 14	330 (57)	283 (10)	321 (48)
Hungarian rail syst. 48	76	40	314 (41)	373 (100)	500 (227)	309 36	368 (95)	363 (90)	312 (39)

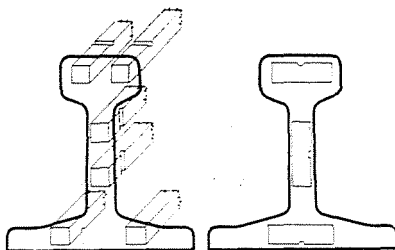


Fig. 12. Cut-out locations of longitudinal and cross specimens for impact tests

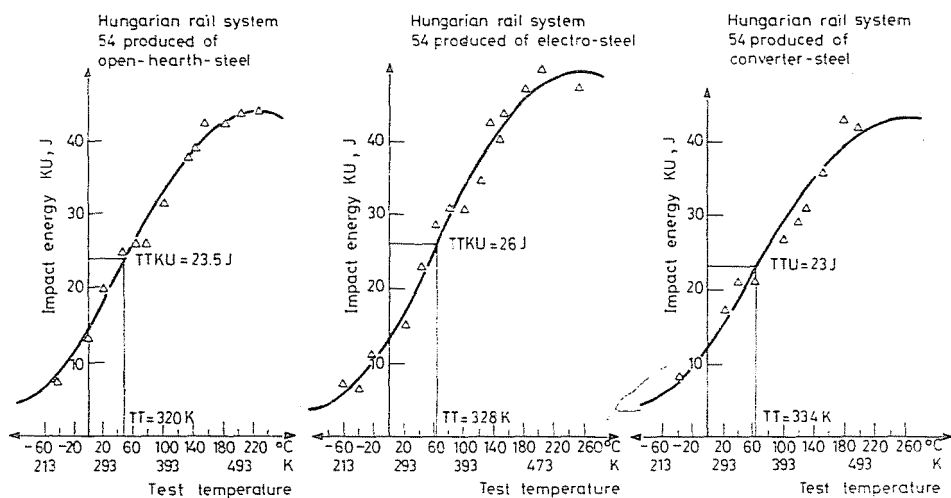


Fig. 13. $KU = f(T)$ curves of Hungarian rails

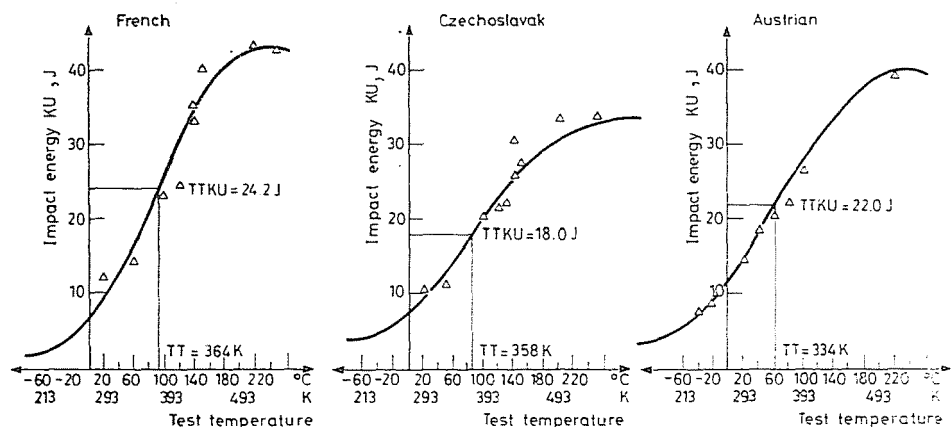


Fig. 14. $KU = f(T)$ curves of foreign rails

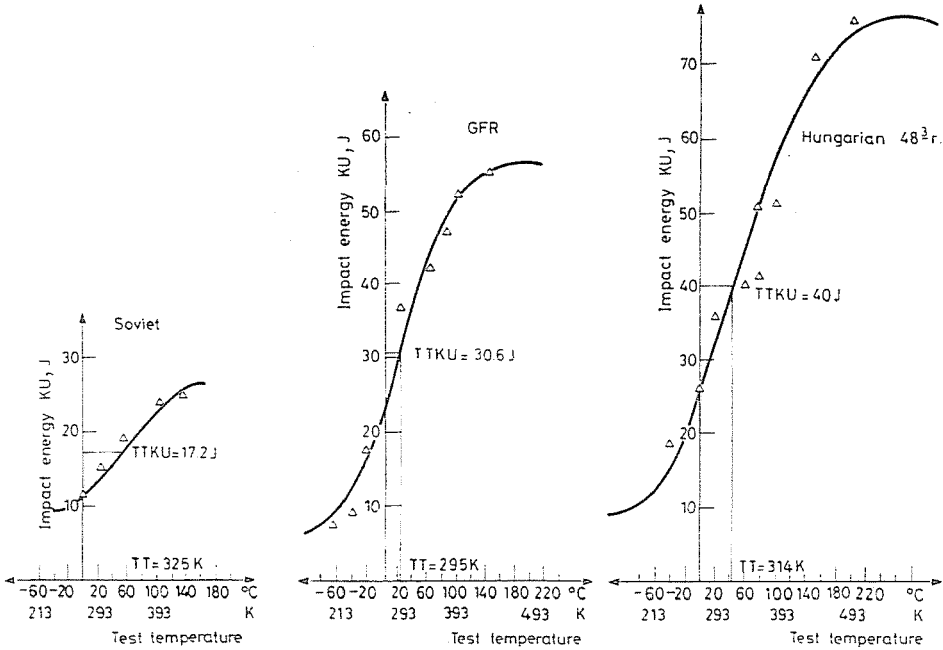


Fig. 15. $KU = (T)$ curves of rails of Hungarian and foreign origins

On the horizontal and vertical axes of the figure the transition temperature ($^{\circ}\text{C}$) and the tensile strength (R_m , MPa) respectively, of the rail are represented. From the figure it is to be seen that the increase of the tensile strength involves the rise of the transition temperature of the rail. The interdependence between the tensile strength and the transition temperature (at the point of inflexion) can be verified both in connection with the Hungarian and foreign rails.

7. Fatigue test of rails

The load repeatedly applied on the track may cause the fatigue and failure of the rail. The research investigation of the rail is particularly significant from the point of view of the safe operation of the railway.

Under laboratory conditions the cycle per second (N) causing failure of the rail is to be determined from which the fatigue limit of the rail steel might be concluded.

The fatigue limit is a stress always lower than the yield point of the rail steel; a somewhat higher stress than that applied repeatedly, causes fatigue failure of the rail but, under the effect of a lower endurance stress than the fatigue limit, failure practically never can occur.

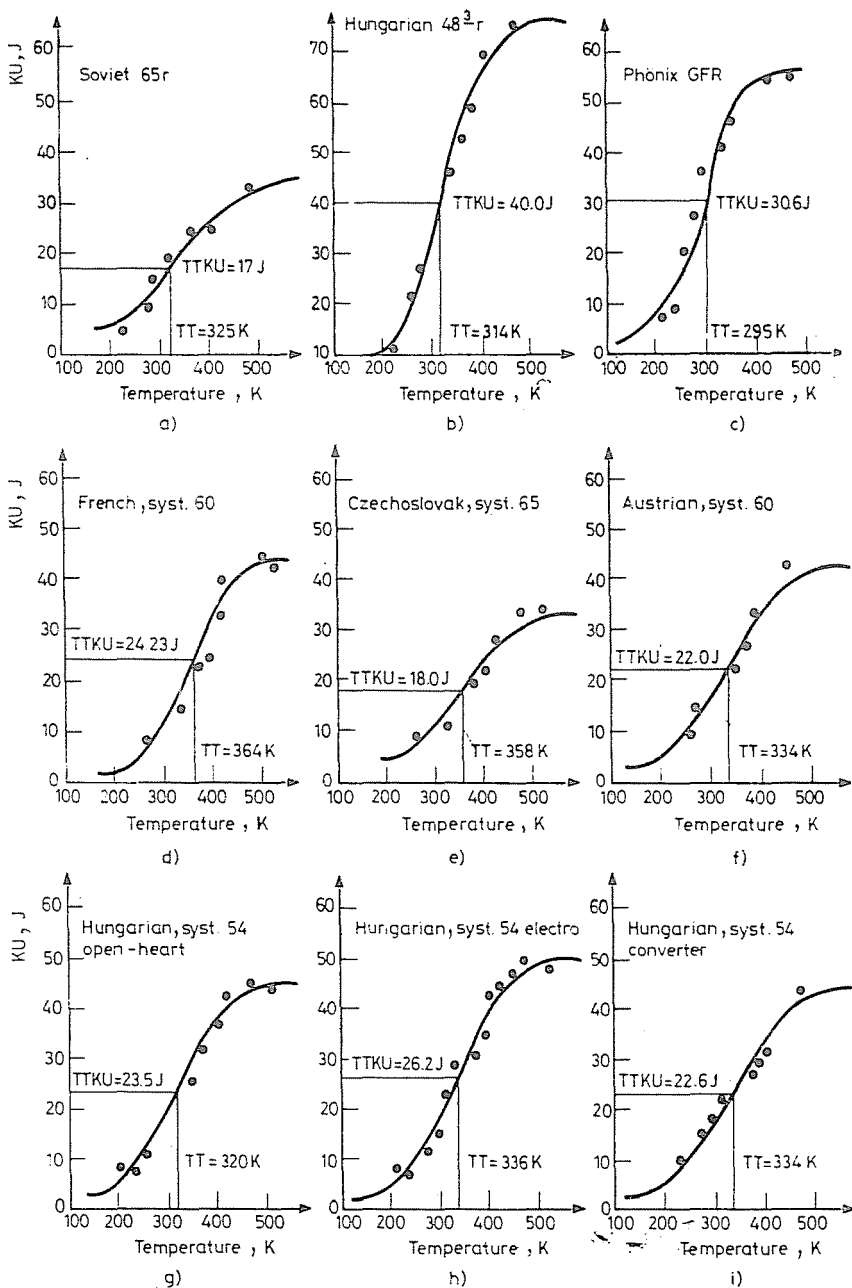


Fig. 16. $KU = f(T)$ curves with values TT and $TTKU$ of rails of Hungarian and foreign origins

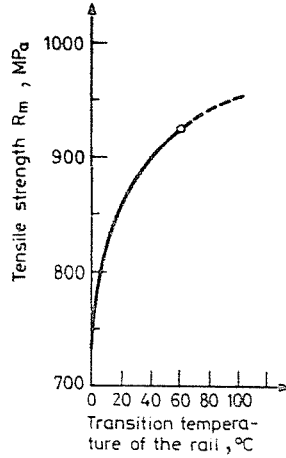


Fig. 17. Development of the transition temperature of the Hungarian rails in dependence of the tensile strength

The characteristic variations of the stress caused by the fatigue load are shown in Fig. 18. In case of oscillating and vibrating endurance tests the specimen is submitted to a stress or deformation of a given amplitude. There can be also performed tests of random nature programmed, simulating the effects of the actual operation conditions.

With the reduction of the stress amplitude, the amount of cycles causing failure increases. After further reduction of the amplitude, at reaching a certain low value, the fatigue limit of the material becomes of decisive significance, the endurance load falls in the safety region.

Fatigue tests of low cycles ($N < 10^4$) and high cycles ($N \geq 10^7$) can be distinguished. In case of fatigue test of low cycles a much larger deformation can be permitted than in case of testing with high cycles.

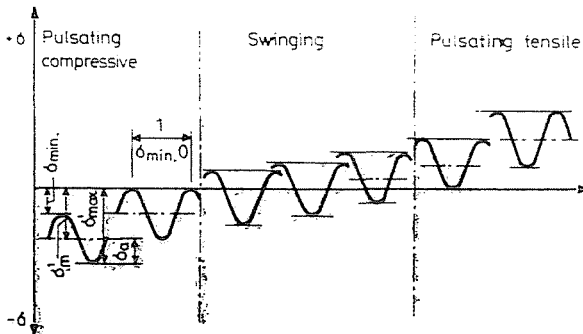


Fig. 18. Typical changes in stresses during endurance tests

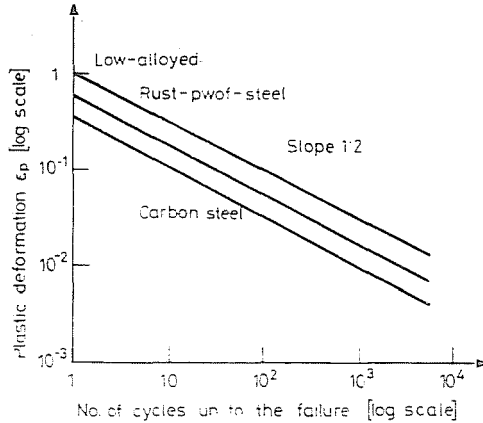


Fig. 19. Interdependence between the plastic deformation and failure at the low-cycle endurance test

On the basis of the fatigue of low cycles the fatigue limit can be well defined with the aid of the relationship (Fig. 19):

$$N = C\varepsilon_p^{-n}$$

wherein:

- ε_p — plastic deformation amplitude,
- n and C — constants of material.

In case of high cycle examinations the non-homogeneous composition or texture as well as the quality of the surface decisively affect the value of the fatigue limit.

The first procedure to definition of the fatigue limit has been worked out by WÖHLER which is used also in these days. Since then a special discipline and a new practice for material testing, the theory and practice of limit-design have been developed which deals with the investigation of service life of materials.

The implement of laboratory did not permit but to apply in investigating the rail steels, the traditional procedures. In case of the Wöhler tests the specimens have been submitted to repeated load, in the case in question to rotary-bending fatigue tests. The number of cycles causing failure is represented firstly in logarithmic and later semi-log diagrams in Fig. 20. The lower horizontal tangent of the fatigue curve cuts out on the stress-axis the fatigue limit associated with the 50 per cent probability of failure.

The stress limits coordinated to the lower probability have been determined with the mathematical procedure to be seen in Fig. 21.

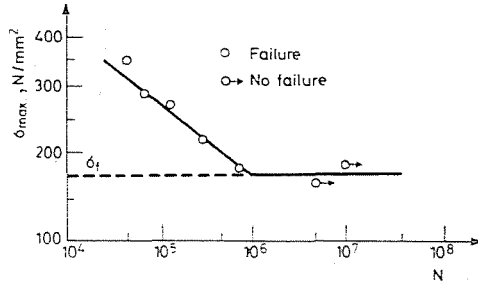


Fig. 20. Double logarithmic Wöhler's diagram

The fatigue test gives a result the more safe the more specimens could be tested at the same levels of stresses and the more levels of stresses could be utilized. Therefore, very many specimens and testing machines are needed.

Be the above conditions restricted, so accelerated fatigue tests worked out appropriately are disposable for the establishment of the fatigue limit (PROTT, LOCATI . . .).

The fundamental principle of the fatigue tests of shortened duration was the assumption related to the superposition of the damages worked out by PAIMGREN and MINER according to which the amount of the work needed to the fatigue failure is always the same, no matter the tests have been performed at a single level or at several levels of stress. The work performed in the course of the endurance tests is proportional to the stress and the number of load repetitions. At the different tests the damages caused on several stress levels are summarized and, according to the theory the failure takes place, as a result of the loads of different levels at the moment where the equality

$$\sum_{i=1}^k \frac{n_i}{N_i} = 1$$

related to the stress levels $\sigma_1, \sigma_2, \dots, \sigma_k$ is valid, wherein:

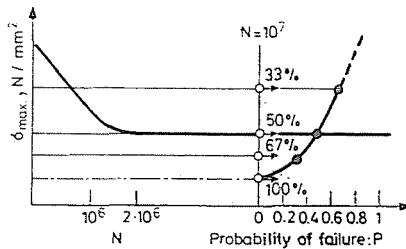
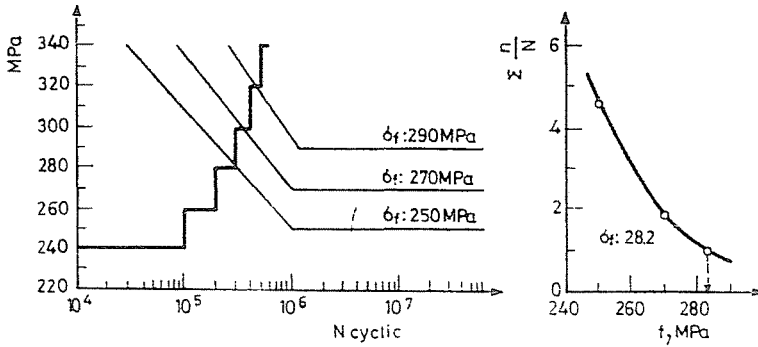


Fig. 21. Experimental determination of the fatigue limit associated with the failure of zero probability



Force MPa	No. of fluctuation n	Stress levels					
		Curve F 250MPa		Curve F 270MPa		Curve F 290MPa	
		N	$\frac{n}{N}$	N	$\frac{n}{N}$	N	$\frac{n}{N}$
240	$1 \cdot 10^5$	∞	o				
260	$1 \cdot 10^5$	$7.05 \cdot 10^5$	0.1418	∞	o		
280	$1 \cdot 10^5$	$3.4 \cdot 10^5$	0.2941	$7.2 \cdot 10^5$	0.1388	∞	o
300	$1 \cdot 10^5$	$1.55 \cdot 10^5$	0.6451	$3.6 \cdot 10^5$	0.2777	$7.2 \cdot 10^5$	0.1388
320	$1 \cdot 10^5$	$0.7 \cdot 10^5$	1.4285	$1.75 \cdot 10^5$	0.5714	$3.7 \cdot 10^5$	0.2702
340	$0.815 \cdot 10^5$	$0.39 \cdot 10^5$	2.0897	$0.88 \cdot 10^5$	0.9261	$19 \cdot 10^5$	0.4289
Damages superposed			4.5992		1.914		0.8379

Locati's procedure applied to GFR-rail
 $n = 1 \cdot 10^5$
 $\Delta\sigma = 20 \text{ MPa}$

Fig. 22. Locati's procedure adapted to the converter rail $n = 4 \cdot 10^5$
 $\Delta\sigma = 20 \text{ MPa}$

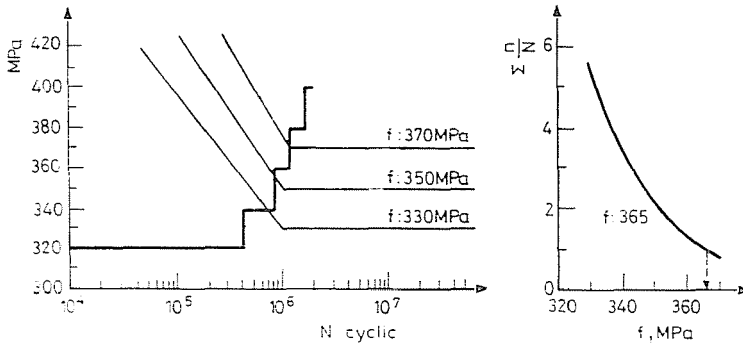
N_i — applying number of loads causing failure at the different stress levels,

n_i — number of application of loads causing damages at different levels of stress (serving for basis to selection).

On the basis of this assumption LOCATI worked out a quick fatigue test, by using of which by applying a load increased step-by-step on a single specimen the fatigue limit can be determined in a short time with an accuracy of 5 to 6 percent.

This method has been applied in the laboratory since for the comparative tests only a few specimens were available from the rails of foreign origin. On the basis of data obtained from the foreign literature on the subject the estimated fatigue limits of the rail steel has been plotted as well as the fatigue curves assuming higher and lower limits.

The specimens have been loaded in the fatigue tests in a stepwise way as is seen on Figs 22 and 23.



Force MPa	No. of fluctuation n	Stress levels					
		Curve F 330 MPa		Curve F 350 MPa		Curve F 370 MPa	
		N	$\frac{n}{N}$	N	$\frac{n}{N}$	N	$\frac{n}{N}$
320	$4 \cdot 10^5$	∞	o				
340	$4 \cdot 10^5$	$7.05 \cdot 10^5$	0.5674	∞	o		
360	$4 \cdot 10^5$	$3.5 \cdot 10^5$	1.1429	$7.1 \cdot 10^5$	0.5674	∞	o
380	$4 \cdot 10^5$	$1.78 \cdot 10^5$	2.2472	$3.65 \cdot 10^5$	1.0959	$7.2 \cdot 10^5$	0.5555
400	$128 \cdot 10^5$	$0.9 \cdot 10^5$	1.4222	$1.88 \cdot 10^5$	0.6809	$4.0 \cdot 10^5$	0.3200
Damages superposed			5.3797		2.3401		0.8755

Fig. 23. Results of fatigue test of short duration performed with the aid of Locati's procedure in testing of service life of rails

7.1 Selection of the stress steps in testing the rails for their service life and the results obtained

To the service life of the rails from the results of the rotary-bending fatigue test can be concluded.

In cases treated of in the present paper the fatigue tests have been performed by applying the shortened Locati-process.

In selecting the stress steps in case of the rails of low tensile strength, as the GFR-Phönix and the Hungarian 48³ rails produced on the open-hearth process, the following values have been assumed:

$$\begin{aligned} \sigma_{f_1} &= 250 \text{ MPa (25 kp/mm}^2\text{)}, \\ \sigma_{f_2} &= 270 \text{ MPa (27 kp/mm}^2\text{)}, \\ \sigma_{f_3} &= 290 \text{ MPa (29 kp/mm}^2\text{)}. \end{aligned}$$

For the majority of the rails tested of eutectoidal texture (both in case of the Hungarian and foreign rails) the assumed stress levels are as follows (Fig. 22):

$$\begin{aligned} \sigma_{f_1} &= 330 \text{ MPa (33 kp/mm}^2\text{)}, \\ \sigma_{f_2} &= 350 \text{ MPa (35 kp/mm}^2\text{)}, \\ \sigma_f &= 370 \text{ MPa (37 kp/mm}^2\text{)}. \end{aligned}$$

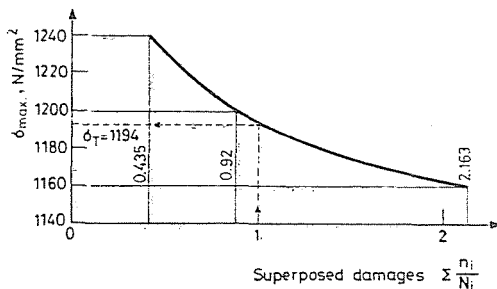


Fig. 24. Determination of the fatigue limit with the aid of Locati's procedure

However, the above latter rails of system 54, 60 and 65 have been made with up-to-date process having higher tensile strength than the previous.

After testing with repeated load $N = 4 \cdot 10^5$ and $1 \cdot 10^5$ the initial load has been increased by 20 MPa up to the failure of the specimen.

The steps of load are indicated in the fatigue diagram. The failure values associated with the load steps and to be read on the three fatigue curves have been summarized in a table and the damages $\frac{n_i}{N_i}$ calculated. The damages belonging to the individual fatigue curves have been added and from the values

$$\sigma_i = \Sigma \frac{n_i}{N_i}$$

belonging together a secondary diagram has been plotted which is to be seen in Fig. 24.

According to the theory of damage the straight line $\Sigma \frac{n_i}{N_i}$ cuts out on the fatigue curve the fatigue limit of the material.

From Table VI is to be seen that the fatigue limit of the rails produced in Hungary is the same as those of the foreign rails involved in the comparison. The fatigue limit calculated σ_f (MPa) does not show a wide scatter.

The respective values of the Hungarian electro, converter and open-hearth-steel rails are as follows

$$\sigma_f: 357; 365 \text{ and } 363 \text{ MPa}$$

In the the case of the Czechoslovakian and French rails these values are 365 MPa, which agree with that of the Hungarian rails made in converter.

The σ_f -value of the Austrian rail is 354 MPa, which is the lowest. The tensile strength of these rails lies between 901 and 952 MPa.

The fatigue limit of the rail GFR-Phónix is 282 MPa and that of the Hungarian rail system 48³ made of open-hearth-steel is 285 MPa, however, their tensile strength are 750 and 882 MPa respectively.

The damages superposed are
in case of the Hungarian rails:
(according the order of succession:
electro, converter and open-hearth-steel):

$$\begin{aligned}\sigma_{f_1(220)} &: 3.63, 5.38 \text{ and } 4.96, \\ \sigma_{f_2(250)} &: 1.66, 2.34 \text{ and } 2.18, \\ \sigma_{f_3(275)} &: 0.60, 0.88 \text{ and } 0.79,\end{aligned}$$

in case of the foreign rails (no fatigue tests have been carried out with the Soviet rails) the damages are as follows (in the order of succession: Czechoslovakian, French and Austrian rails):

$$\begin{aligned}\sigma_{f_1(220)} &: 3.14, 3.27 \text{ and } 3.78, \\ \sigma_{f_2(250)} &: 1.73, 1.71 \text{ and } 1.49, \\ \sigma_{f_3(275)} &: 0.88, 0.85 \text{ and } 0.52.\end{aligned}$$

Considering the fatigue limits and the damage values superposed and compared with the values of the tensile strengths, the Hungarian rails furnished favourable results.

Table VI

Results of rotary-bending fatigue tests obtained by making use of Locati's method

Origin	stress level (MPa)			$\Delta\sigma$ MPa	No of repeated loads (N)	Fatigue limit calculated (σ_f) MPa
	σ_{f_1}	σ_{f_2}	σ_{f_3}			
	330	350	370			
damages superposed						
electro	3.6282	1.6615	0.5957	20	$4 \cdot 10^5$	357
converter	5.3797	2.3401	0.8755	20	$4 \cdot 10^5$	365
open-hearth-steel	4.9642	2.1836	0.7900	20	$4 \cdot 10^5$	363
Czechoslovak	3.1413	1.7258	0.8771	20	$4 \cdot 10^5$	365
Austrian	3.7845	1.4891	0.5223	20	$4 \cdot 10^5$	354
French	3.2676	1.7141	0.8490	20	$4 \cdot 10^5$	365
Soviet	—	—	—	—	—	—

Origin	Stress level (MPa)			$\Delta\sigma$ (MPa)	No of repeated loads (N)	Fatigue limit calculated (σ_f)
	σ_{f_1}	σ_{f_2}	σ_{f_3}			
	250	270	290			
damages superposed						
GFR (Phönix)	4.5992	1.9140	0.8379	20	$1 \cdot 10^5$	282
Hungarian open-hearth-steel	4.8224	1.7236	0.7462	20	$1 \cdot 10^5$	285

As a matter of course, the above results were obtained by rotary-bending fatigue tests which, in case of the railway rails is not the most characteristic pattern of endurance load. The adoption of pulsators of high performance, up-to-date material-testing equipments and processes will widen and make more exact the knowledge in relation of the fatigue behaviour of the rails.

8. The origin and propagation of fatigue cracks in the rail head

Fatigue cracking takes place at faulty locations submitted to concentrated stresses. The geometric transitions in the rail cross section do not play any role, in general, in giving rise to cracking.

It may occur that the intercrystalline stress and an overload simultaneously cause failure. An overload can give rise to a fatigue crack. A stress concentration at a local defect is sufficient to give rise to the propagation of a crack merely under the effect of the load of normal operation. Under the process of the fatigue load an initial micro-crack increases. *In case of a fatigue crack the high local stresses give rise to the plastic deformation or the material locally will be crushed.*

After the origin of the crack, the occurrence of the failure depends on the quickness of the development or increase of the cracking. The rail cracked is still for a long time safe in service if the load remains beneath that which caused the rise of the crack. It can also occur that the crack does not propagate until a further overload does not occur. The extent of the propagation of a crack depends on

- the load applied,
- the inner defects of the material.
- the inclusions and
- on the fatigue limit.

The development of a crack is proportional to the load. Under a higher load the crack increases quicker. Such a load is also imaginable under which the fatigue crack takes its origin, however, it does not propagate because the load remains beneath that earlier applied.

The propagation of the crack depends also on the way of application of the load. In case of a tensile endurance test the stress distribution in a cylindrical specimen is uniform. In case of bending, the stress distribution is non-uniform, the inner fibres are braking, the slipping of the outer fibres are supported by the inner ones.

Under the effect of tensile load of the same magnitude, the propagation of the cracks is quicker than under flexural load.

To the fatigue crack it is representative that it is initiated from the inward one third part of the cross section of the rail head, and propagates in all directions, then

developing on the whole cross section of the rail head calls forth failure. If the oval flaw develops to failure, the *failure of flaw-type takes place*.

The oval-type fatigue flaw represents a significant latent danger, because it is of cross direction and remains imperceptible until it appears on the surface.

At the moment of the appearance on the surface the flaw is extended already on a large part of the cross section of the rail head and the failure of the rail takes place under the effect of a dynamic load lower than the average. *The danger of this type of flaw is increased by the fact that it can occur in many cases in a rail in a dense succession.* In case of flaws lying in close neighbourhood to each other, failures can occur at each flaw and *pieces of rail can be broken out.* *Such failures can cause derailments.* (E.g., in Hungary, near Csór—Nádasladány a length of rail 3.5 m has been broken into 13 pieces.)

The oval-type fatigue rail failure is now a new phenomenon, however, ten years ago it occurred frequently in the tracks of the MÁV, *even in case of rails of high grade production.* In that period the oval-type fatigue flaw represented a *serious danger to the safety of railway operation.*

The railways in performing research investigations on the origin of fatigue flaws made use of the most up-to-day methods. Unfortunately, these investigations did not bring unequivocal results, the *ascertainments made were based on assumptions.* Until being able to eliminate this type of deficiency only the application of a systematic, non-destructive testing gives a satisfying assistance against failures. With the modernization of the railway lines and with the increase of loads the deficiencies in question have been multiplied, however, by applying a systematic supervision the accidents became to be avoided.

8.1 *The fatigue oval flaw and failure in the rail head*

The *fatigue*, thereafter the failure, whether hard or soft, are caused by an *effect connected with crystalline deficiencies.* In these processes both the point-type and the one, two and three dimensional deficiencies might be taken into consideration. It may be noted that the polycrystalline iron material contains a great number of mosaic limits and crystallite limits (two-dimensional faults), contaminating atoms and Frenkel-deficiencies (faults of zero dimension), inclusions (three-dimensional faults), dislocations (one-dimensional faults), etc. It has to be taken into account also that the plastic deformation intervening during processing or later, leads to mechanical bimetalization by creating the bimetal limits.

To the starting of cracks *several alternative process can contribute*, such as:

a) *initially existing micro-inclusions*; in the course of rolling an *inclusion-cavity* exists at the point of development in the neighbourhood of which a *stress space comes into being*;

b) *oscillation movement of dislocations* under the cyclic load in the environment of the hang. The moving dislocation gives rise to *point deficiencies* and by

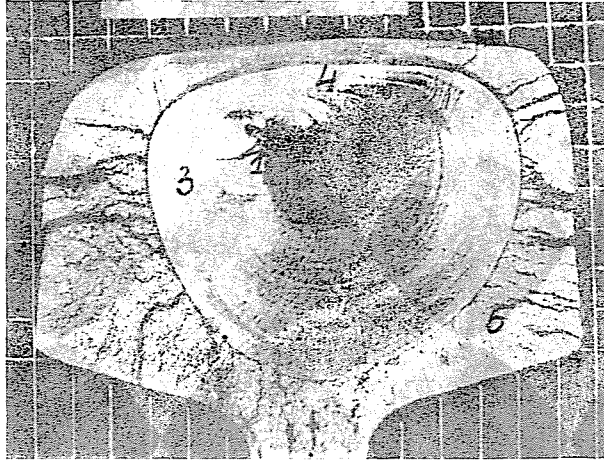


Fig. 25

this locally spoils the *order of the crystallization*. Condensation of the defective spots or high concentration of the interstitial atoms can create such stress field which *generates micro-fissures*;

c) in the rail head the resultant stress is higher than at other locations of the cross section; due to the higher stress local plastic deformation takes place, *in the micro-crystal a great number of hanged series of dislocations arise the energy and interaction of them give rise to fissures*.

Flakes existing at the production arranged *parallelly to the longitudinal axis of the rail do not give rise to fatigue oval flaw* in general, and to their turning into the cross position there is but a little possibility.

Accordingly, the cause of the fatigue failure is to be found in all likelihood in the processes of the dislocations.

In summing up the actual situation it should be taken into account that it is to be dealt with a polycrystalline metal which, beside the dislocations contains a great number of crystalline deficiencies the effect of which can make the process to be more intricate.

By examining the surface of the fatigue failure with the aid of a stereomicroscope it can be established that it is composed of four parts (Fig. 25) as follows:

a) the nodule where later in the operation the oval flaw starts. This is of brittle-fracture nature with a crystalline brilliant surface. The fracture is wavy, uneven, it does not fit to a plane. Its size is variable upwards from a size of a pinhead.

b) The surface of the oval flaw; according to the macro and micro examinations several fatigue cracks which started according to concentric pattern from the nodule lying nearly in the same plane.

c) A sharp incision between the oval fatigue flaw surface and the extreme (outer) surface.

d) Finally the outer failure surface reminding to a brittle fracture of crystalline scintillation.

The first two defective surface and the third sharp incision can weaken the cross section of the rail to such an extent that the fourth failure surface comes into being abruptly in consequence of a sudden fracture.

On the smooth surface of the fatigue field projecting boundary lines can be observed resembling to contour lines, regularly arranged, reminding to annular rings. Their arrangement demonstrates the propagation of the crack. These signs are those referring to fatigue limit, or load limit. The limiting signs are generated by the loads, respectively their interruption.

Loads which are higher and lower than the fatigue limit result in fractures where on the marks of load boundaries can be observed.

The stress concentration taking place in the rail head makes the stress distribution to change, the tensile stress will be multiplied while the shear stress remains in essential unchanged. In this way, the tensile stress reaches earlier the tensile strength than the shear stress reaches the shearing strength of the material.

According to an other opinion, occurrence of the oval fracture of the rails is a result of two processes. One of the two processes involves the period of coming into existence of the crack, i.e., the appearance of the cracks of macroscopic size. In this period, in case of a given external load there are the texture of the rail steel, i.e., its content of inclusions, their nature and quantity which are of definite significance. Keeping between rational limits the above parameters is the common task of the metallurgy and the railway engineering.

The second period of the process leading to the failure of the rail the steady propagation of the macroscopic crack up to the moment where its extension attains the critical value at which the failure takes place under the effect of a single load.

As is to be seen from that said above to the estimation of the endangerment involved in the crack such a characteristic of the rail-material behaviour is needed which mirrors the resistance to the propagation of the fatigue crack of the rail steel.

8.11 *The conditions of propagation of the fatigue crack in the rail steel*

The resistance to propagation of crack in a material can be defined by the change in length of a crack of a given extent during a load cycle. That is, at one side stands the velocity of propagation of the crack, i.e., the change in length per load cycle da/dN and on the other side such a value should stand which beside the load (i.e., nominal stress) involves also the instantaneous length of

the crack. Between the velocity of propagation of the crack and the coefficient of the intensity of the stress a relation of the form

$$\frac{da}{dN} = C(K^n)$$

can be written wherein C and n mirror the behaviour of the material. This expression has been established by Paris and Erdogan. The propagation of the crack accelerates at the end of the cycle, hereafter reaches a critical value, and the failure takes place.

From the point of view of the practice it is the second phase of the propagation of the crack which can be utilized the best and which characterizes the best the behaviour of the rail steels. Here, the values of C and n depend on the chemical composition and mechanical properties of the rail. This solution is to be applied only in case where the value of the coefficient of the stress intensity is familiar. However, the computer programs needed to this way of solution are not disposable. But one could take a risk also to maintain the value of uncertainty which, however, must not be accepted.

The fatigue tests performed up the failure on rail sections containing actual defects which have been used for a few years, might be considered more advantageous.

8.2 Location, form, size of the fatigue oval flaws and the surface of fracture

The centre of the fatigue oval flaw (Fig. 25) in the rail head beneath the running surface takes place at the one third and two third part of the height. According to the measurement results the upper border of the occurrence lies in a non-worn rail at a distance *about 11 mm and the lowest border at 24 mm beneath the running surface*. Thus the place of the nodule in vertical sense is defined.

The *nodule* is accordingly *above the web and beneath the running face of a width of about 21 mm which, from the point of view of the supersonic test is advantageous*. The supersonic sound waves arriving from the test head into the rail head can touch the tiniest defect which, from the point of view of safe operation is the sine qua non of the detection of a defect at the right time.

By *examination of the fracture* with the aid of a stereo-microscope it can be established that it is composed of four parts (Fig. 25) as follows:

a) the centre *nodule* from which the oval fatigue later developed. It has the *character of a brittle fracture*, in general, of a surface of *crystalline scintillation*. The surface is *wavy, uneven*, does not fit to a plane. Its size is variable upwards from the size of a pinhead.

b) *The oval flaw surface*; according to the macro and micro examinations, *several fatigue cracks which started according to a concentric pattern from the centre lying nearly on the same plane*.

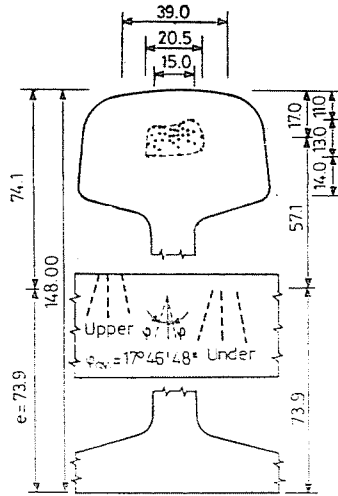


Fig. 26. Location of the nodule of the oval flaw in the rail head

The examinations verified that the fatigue oval flaw and *fatigue oval fracture coming into being from the flaw is perpendicular to the longitudinal centre line of the rail or forms an angle with it*. The defect is, in most cases, deflected from the vertical direction. The angle of deflection lies between zero and 28° , its average value is $17^\circ 46' 48''$, i.e., 18° (Fig. 26).

The form on the cross direction of the fatigue oval flaw is elliptic. The width of the elliptic flaw is according to the measurements, in general, one and a half of the height of it.

Also such defects are to be found, though rarely, where the ratio of the height and width is 1:1 or 1:2. The extent and development of the defect is represented in Fig. 27. The width of the fatigue oval flaw, developed from the centre is proportional to its height.

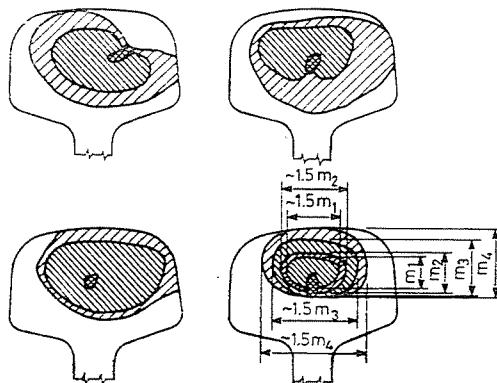


Fig. 27. Ratio of the height and width of the oval flaw

The sketches of the forms of defects have been drawn after actual oval-type fatigue failures of rails which on the basis of the results of supersonic tests have been cut out from the rails lying in the track found to be defective, and have been submitted to fatigue test. On the surfaces shaded differently, the transition developed during the different fatigue cycles. This method of test permitted to conclude to the development of the area of the oval flaw.

The fatigue test has been performed on rails supported in the test equipment with head downwards because in this way the development of the failure from the internal defect was quicker and the results appeared on the safe side. *The load pattern (support and loading force) and the results of the fatigue test permit the safe determination of the service life of the defective rail section.*

8.3 Determination of the extent and calculation of the flaw with the aid of ultrasonic testing

Height and extent of a fatigue oval flaw can be determined. The emissive element of the supersonic tester contains two radiant crystals, one of them irradiates the defect ahead in the direction of the advancement, the other one, passing beyond the defect irradiates it backwards (Fig. 28).

The trajectory S striking against the defect can be read on the cathode-ray tube.

The height of the defect is as follows:

$$m = S \cdot \sin 20^\circ$$

By projecting the length S on the chart and then on the height of the rail head one obtains the height of the defect as well as the depth of it beneath the running surface of the rail (Fig. 28).

Also the inclination of the defect can be defined. At the irradiation to the forward direction, at the moment where the defect appears on the cathode-ray tube the location A of the head of irradiation of the supersonic tester is to be marked on the rail head, thereafter in advancing the detector head and continuing the observation, on the cathode-ray tube the path-length of the ray will be seen, and then the detector head arrives to the point B which also is to be marked on the rail head.

At the opposite side of the defect the points C and D can be defined in the very same way and the value S associated with them can be read on the cathode-ray tube. Here, $\overline{AB} = a'$, $\overline{CD} = d$, $\overline{BC} = 2b'$. Since $\overline{AB} = \overline{CD}$, the defect is inclined at an angle φ to the vertical; $m_1 \neq m_2$, $m_2 > m_1$, because $d > a'$.

With the aid of the angles and projections known, the formula of x can be written considering the two scalene triangles obtained by pushing together the

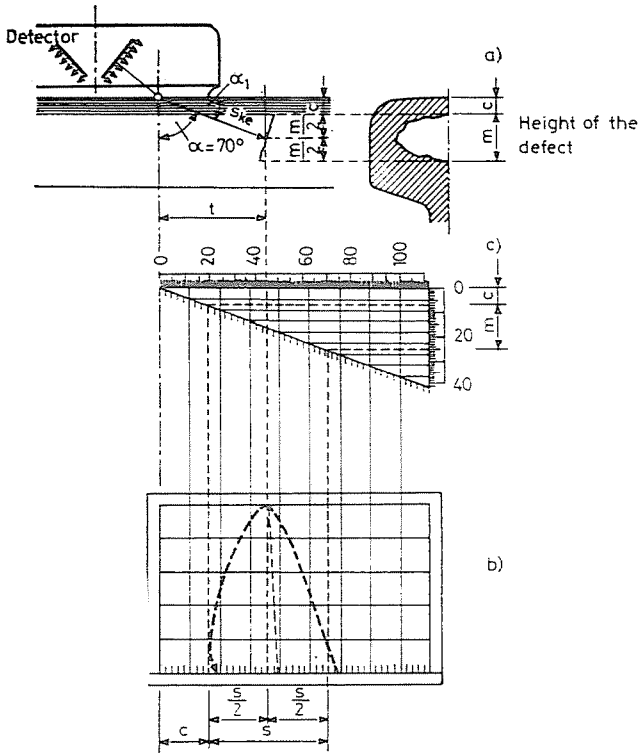


Fig. 28. Definition of the height of the oval flaw

triangles developed at the projections a' and d (Figs 29, 30):

$$x = a' \frac{\sin \alpha_1}{\sin (90^\circ - \varphi - \alpha_1)}$$

After performing the different operations one obtains:

$$\operatorname{tg} \varphi = \operatorname{ctg} \alpha_1 \frac{d - a'}{d + a'}$$

By knowledge of the angle φ , the value of the defect of height x can be calculated with the aid of the formula which after deduction reads as follows

$$x = a' \frac{\sqrt{\sin^2 \alpha_1 + \cos^2 \alpha_1 \left[\frac{d - a'}{d + a'} \right]^2}}{\cos \alpha_1 \cdot \left[1 + \frac{d - a'}{d + a'} \right]}$$

After reduction

$$\cos \varphi = \frac{m}{x}$$

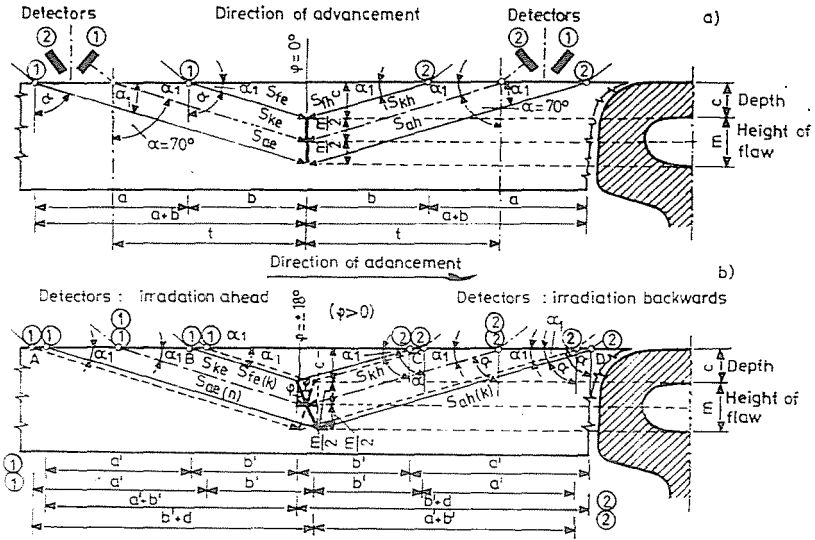


Fig. 29. Searching for the oval flaws by supersonic method

with φ = angle of inclination of defect to vertical direction,
 m = height of projection of defect,
 x = actual height of defect.

The height of the defect is given by the formula in knowing the distance between the projections

$$m = \frac{a' + d}{2} \cdot \operatorname{tg} \alpha_1.$$

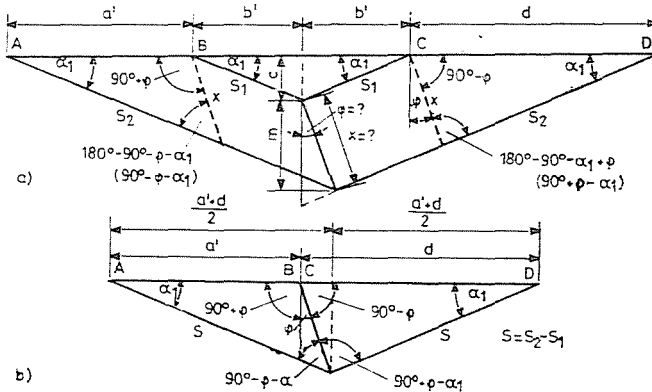


Fig. 30. Inclination and height of the oval flaw

By calculations tables may be established or charts could be plotted to carry out actual works and to the estimation of the dangerous nature of the fatigue oval flaw of the rail.

8.4 Development and calculation of the fatigue oval flaw in dependence on the gross ton load

The rail sections containing oval flaw defects have been cut out from the track and subjected to a test of further fatigue load. In the fatigue tests the rail specimens have been put into the endurance testing machine, supported head downwards with a span 0.8 m which was the maximum on the test machine disposable, correspondingly to the stresses caused, in general, in the rail by the normal operation. Between stopping and restarting the fatigue test, the defect has been repeatedly inspected by supersonic examination, the extent of its development determined and the results obtained recorded.

In order to obtain the minimum, the partial derivative with respect to a_1 and b_1 has to be equalled to zero.

$$\frac{\partial}{\partial a_1} \sum_i (a_0 x_i e^{b_0 x_i} b_1 + e^{b_1 x_i} a_1 + \dots - z_i)^2 = 0$$

The data yielded by the endurance test in connection with the load and the development of the area of the flaw are to be plotted and the most dangerous points of propagation are to be taken for basis for the calculation. The determination of the area of the flaw has been carried out with the aid of planimetry on photograph, after the failure of the rail.

In order to be able to treat of in a simpler form the propagation of the flaw the equation of the curve plotted, has been established in dependence on the propagation of the area of the flaw and the gross tons passed upon it. The form of the formula has been selected with the aid of the procedure of linearization.

It has been assumed that between x and y the following functional connection is valid

$$y = ae^{bx} + c.$$

Let us introduce the new variables $X = x$ and $Y = \log(y - c)$; between them the following linear relation is obtained:

$$\log(y - c) = \log a + b X \log e.$$

In case where the functional connection $y = ae^{bx} + c$ subsists, the calculation of $X(x)$ and $Y(y)$ shows that this relationship is linear. The parameters of the function have been determined with the aid of the method of least squares,

however, first approximate values have been calculated. The approximate values of the parameters have been established with the aid of six points on whose basis:

$$\begin{aligned} a_0 &= 13 \\ b_0 &= 0.05 \\ c_0 &= -a_0 = -13 \end{aligned}$$

The parameters are:

$$\begin{aligned} a &= a_0 + a_1 \\ b &= b_0 + b_1 \\ c &= -a \end{aligned}$$

Consequently the function reads as follows:

$$y = (a_0 + a_1)e^{(b_0 + b_1)x} - (a_0 + a_1) = a_0e^{b_0x} + a_1e^{b_1x} - a_0 - a_1$$

Expanding e^{b_1x} in power series and introducing the designation $z = y - a_0e^{b_0x} - a_1$ yield a relationship which, considering the measurement data, contains the unknown values (x_i, y_i, z_i) a_1, b_1 .

The solution to the set of equations is circumstantial, therefore, it is convenient to find a solution at which the square-sum of the equation gives the minimum.

$$\sum_i \left[\left(a_0x_i e^{b_0x_i} b_1 + e^{b_0x_i} a_1 + x_i e^{b_0x_i} a_1 b_1 + \frac{1}{2} - a_0x_i^2 e^{b_0x_i} b_1^2 + \right. \right. \\ \left. \left. + \frac{1}{2} - x_i^2 e^{b_0x_i} a_1 b_1^2 - a_1 \right) - z_i \right]^2$$

and

$$\frac{\partial}{\partial b_1} \sum_i (a_0x_i e^{b_0x_i} b_1 + e^{b_0x_i} a_1 + \dots - z_i)^2 = 0$$

After derivation, a_1 and b_2 which are very small values, retaining only the linear terms and carrying out the possible reduction one obtains:

$$\sum_i (e^{2b_0x_i} - 2e^{b_0x_i} + 1) a_1 + \sum_i (a_0x_i e^{2b_0x_i} - x_i z_i e^{b_0x_i}) b_1 = \sum_i (z_i e^{b_0x_i} - z_i)$$

and

$$\begin{aligned} &\sum_i (a_0x_i e^{2b_0x_i} - a_0x_i e^{b_0x_i} - x_i z_i e^{b_0x_i}) a_1 + \\ &+ \sum_i (a_0^2 x_i^2 e^{2b_0x_i} - a_0 x_i^2 z_i e^{b_0x_i}) b_1 = \sum_i a_0 x_i z_i e^{b_0x_i} \end{aligned}$$

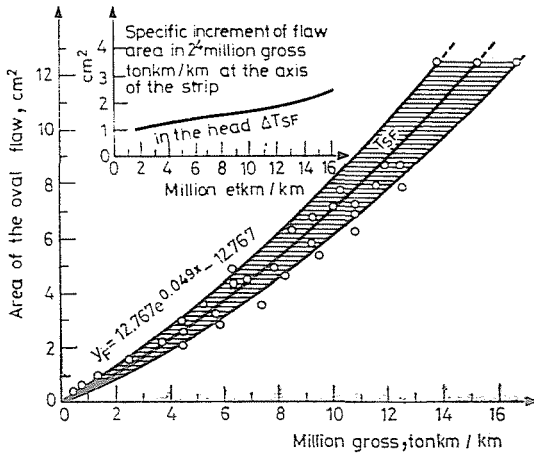


Fig. 31. Expansion of the flaw surface in the head

The solution to the set of equations gives:

$$a_1 = -0.233265$$

$$b = -0.000637$$

and

$$a = a_0 + a_1 = 13 - 0.233265 = 12.766735$$

$$b = b_0 + b_1 = 0.05 - 0.000637 = 0.049363,$$

wherefrom the approximate function is (Fig. 31):

$$y = 12.7667 \cdot e^{0.0494 \cdot x} - 12.7667$$

The permissible extent of the defect in the useful area of the rail head (threshold value) is given by the railways in per cents. According to the French railways the 55 per cent of the cross-sectional area of the rail head is permitted to be defective which means a safety of 95 per cent. In the German Federal Republic a defect of an area of 50 per cent of the rail head is tolerated.

According to the examinations of the Hungarian State railways the defect in the rail head may be of high and low situation. The defect located at the upper part of the rail head significantly reduces the moment of resistance of the rail.

A rail with an area of defect larger than 45 per cent must not be retained in the track. This value is adopted as the threshold value.

By measuring the actual height of the rail, in Fig. 32 the cross-sectional area worn can be read in cm².

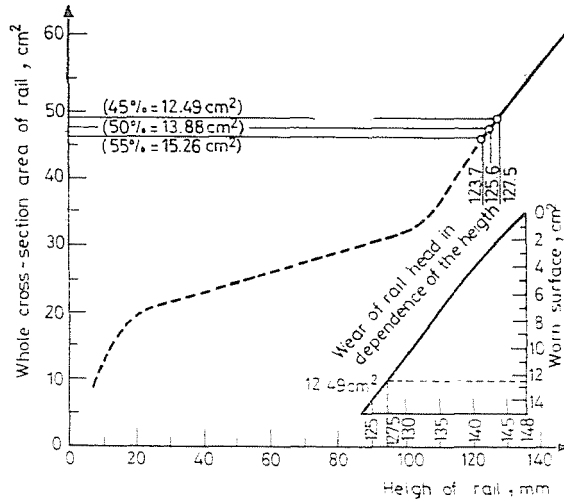


Fig. 32. The area of the rail profile in dependence on the rail height in case of the rail 48³

The height of the oval flaw can be determined with the aid of supersonic test or calculated on the basis of the auxiliary data.

The magnitude of the flaw area in the rail head can be classified into three categories:

a) The area of the defect is larger than the 45 per cent of the area of the rail head, however the flaws are superposed. Superposition is assumed in case where the defects are nearer than the distance of three or five sleeper-spacings.

An uneven number of spacings are taken into consideration because the propagation of the waves of oscillation becomes zero in this way above the supports and the number of the uneven supports (sleepers) mean a whole wave. In case of a track of continuously welded rails maintained in a sound condition where the spacings of the sleepers are 60, 65 cm, the distance between the defects is 180 to 195 cm. In case of a track maintained in a poor condition, it is convenient to include five spacings of sleepers into the calculations. In case of spacings of 77 cm the lengths will be longer, however, the above assumption yields results on the safe side, which is more favourable than the 2.0 m established uniformly. The rail containing superposed defects is to be replaced immediately. It should be proceeded in the same way in case where the area of the flaw attains the 45 per cent of the cross-sectional area of the rail head.

b) The extent of the flaw falls between 20 to 45 per cent of the cross sectional area of the rail head. In this case it is convenient to play for safety, the gross tons rolling over per month and their effect in increasing the extent of the defect should be defined. In case where the flaw does not reach the 45 per cent until the next non-destructive examination, the rail can be left remaining in the

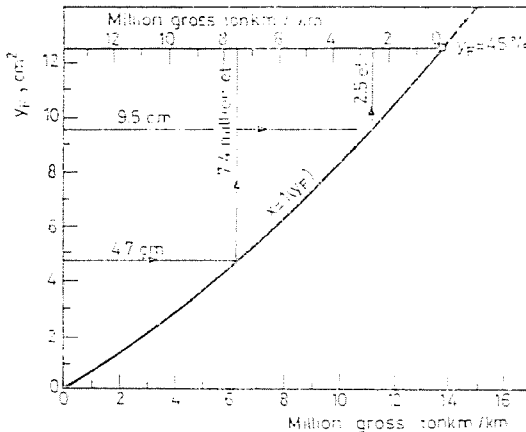


Fig. 33. Development of the oval flaw

track until the term of the next rail examination. Should the development of the defect be estimated to surpass the threshold value before the next rail test, the sum of the permissible gross tons to pass over the defective rail is to be defined, and on the basis of the calculated term of the permissible service the term of the replacement of the rail should be determined.

c) In this category are classified the rails the defect in the head of which does not reach the 20 per cent of the cross sectional area of the rail head. It might be esteemed that the defective rail can be left in dependence on the traffic load to lie in the track until the next rail test. In limiting conditions the calculations mentioned above are also in such cases to be carried out. The chart represented in Fig. 33 serves to define the sum of the gross tons to pass over the defective rail which causes the flaw to reach the threshold value of 45 per cent of the cross sectional rail head.

The sudden-break depth (thickness of the sound cross section under the running surface of the rail, i.e., the distance of the upper edge of the defect to the external surface) is always to be taken into consideration.

In case where the supersonic test detects the defect in a depth of 2 mm from the external surface, the defective cross section is to be strengthened with fish plates or to be cut out.

In defining the extent of the defect, the decrease in height of the rail profile due to wear is also to be taken into account which is to be determined in cm^2 and to be added to the area of the fatigue flaw. The sum of the two areas expresses the magnitude of the lacking area.

The summing up of the areas mentioned above is to be seen on the chart of Fig. 34. With knowledge of the height of the flaw, its area can be read on the curve 1 of the figure, in cm^2 . If the rail profile is not worn, the value obtained is

to be projected to curve 2, the left-hand side of which shows the value of the defect in per cent. On the right-hand ordinate the height of the flaw is to be seen in cm. The small circles on the curves designate the 45 per cent threshold value. The defective area has been calculated in dependence on the height of the defect of elliptic form with a ratio of axes 1.5 : 1.0.

The height of the oval flaw taking place in the rail head and the area of the rail wear are to be summarized as is shown in Fig. 34. First the height of the flaw is to be reported on the right-hand side ordinate of the figure. This value should be projected on curve 1 and the point of intersection to the abscissa, whereby the surface area of the flaw is produced in cm². Adding to this the area of the wear of the rail profile on the abscissa, whereafter projecting the values on curve 2, and directing the point of intersection of them and of the curve to the left-hand side ordinate one obtains the reduced cross sectional area of rail profile in the per cent of the rail head. The figure represents an example to the addition of the flaw and the rail wear.

Dr. Sándor KECSKÉS H-1521 Budapest